

## Reduction of Carbonate Electrolytes and the Formation of Solid-Electrolyte Interface (SEI) in Lithium Batteries. 2. Radiolytically Induced Polymerization of Ethyl Carbonate.

Ilya A. Shkrob<sup>\*1</sup>, Ye Zhu,<sup>1</sup> Timothy W. Marin,<sup>1,2</sup> and Daniel Abraham<sup>1</sup>

<sup>1</sup> *Chemical Sciences and Engineering Division, Argonne National Laboratory, 9700 S. Cass Ave, Argonne, IL 60439*

<sup>2</sup> *Chemistry Department, Benedictine University, 5700 College Road, Lisle, IL 60532*

### Alphabetical list of abbreviations used in the text.

COSY	<sup>1</sup> H- <sup>1</sup> H COrrelation NMR SpectroscopY
DFT	density functional theory
DMC	dimethylcarbonate
DMSO	dimethylsulfoxide
EC	ethylene carbonate
EC(-H)Y	Y-substituted EC at methylene carbon
EO	ethylene oxide, (CH <sub>2</sub> CH <sub>2</sub> O)
EPR	Electron Paramagnetic Resonance spectroscopy
ESI MS/MS	electrospray ionization tandem mass spectrometry
NMR	Nuclear Magnetic Resonance
SEI	solid-electrolyte interface
PC	propylene carbonate
ppm	part per million
rms	root mean squares
TMS	tetramethyl silane
Q	-OCO <sub>2</sub> <sup>-</sup> Li <sup>+</sup> group
VC	vinyleno carbonate
X	either oxygen or carbonate (negatively charged if terminal)

**Scheme 1S.**

Solvolytic and H/D exchange in the terminal and side Q-branches on the polymer chain.

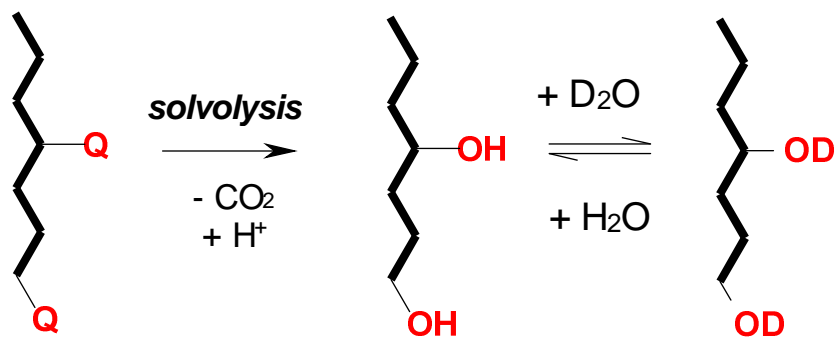


**Table 1S.**

Algorithmic attribution of the loss fragments in ESI MS spectra of EC-*d*<sub>4</sub> in MeCN/D<sub>2</sub>O.

mass (D) a.m.u.	attribution	mass (H) a.m.u.	isobar fraction, %
20 <sup>a</sup>	D2O;	18;	
32 <sup>a</sup>	CD2O;C2D4;	30;28;	83.2;16.8;
36 <sup>a</sup>	CD4O;	32;	
44 <sup>a</sup>	CO2;	44;	
48 <sup>a</sup>	C2D4O;	44;	
52 <sup>a</sup>	C2D6O;C3D8;	46;44;	34.2;65.8;
60 <sup>a</sup>	D6O3;C2D2O2;	54;58;	11.1;88.9;
64	CD2O3;C2D4O2;	62;60;	29.2;70.8;
68	C3D8O;C4D10;	60;58;	18.2;81.8;
76	C2D2O3;C3D4O2;	74;72;	40.4;59.6;
80	C2D4O3;C3D6O2;C4D8O;C5D10;	76;74;72;70;	9.1;13.7;19.9;57.2;
84	C3D8O2;C4D10O;	76;74;	17.2;82.8;
88	C4D12O;	76;	
92	C3D4O3;	88;	
96	CD10O4;C3D6O3;C4D8O2;C5D10O;	86;90;88;86;	12.3;55.7;17.0;15.0;
100	C3D8O3;C5D12O;C6D14;	92;88;86;	46.0;21.2;32.8;
104	C3D2O4;	102;	
108	C2D2O5;C3D4O4;C4D6O3;C5D8O2;	106;104;102;100;	52.5;20.9;16.6;10.0;
	C2D12O4;C3D6O4;C4D8O3;	100;106;104;	
112	C5D10O2;C6D12O;	102;100;	18.1;34.8;7.5;22.0;17.6;
116	C4D10O3;C5D12O2;C7D16;	106;104;100;	32.7;9.6;57.7;
120	C4D4O4;	116;	
124	C2D10O5;C4D6O4;C5D8O3;	114;118;116;	23.1;32.0;44.9;
128	C4D8O4;C7D14O;	120;114;	84.6;15.4;
132	C3O6;C4D18O3;C5D12O3;	132;114;120;	77.5;17.2;5.3;
136	C4D4O5;C5D6O4;C7D18O;	132;130;118;	7.3;63.0;29.7;
140	C3D12O5;C5D8O4;	128;132;	6.5;93.5;
144	C2D12O6;C3D14O5;C6D12O3;C7D14O2;	132;130;132;130;	37.7;24.4;11.7;26.1;
148	C5D20O3;C7D16O2;C8D18O;	128;132;130;	20.5;32.4;47.1;
152	C4D20O4;	132;	
	C4D6O6;C4D14O5;C7D12O3;C8D14O2;	150;142;144;142;	5.9;23.3;14.4;20.3;
156	C8D22O;	134;	36.0;
160	D16O8;C3D14O6;C6D12O4;	144;146;148;	13.1;69.1;17.7;
164	C5D20O4;	144;	
	C4D20O5;C5D6O6;C5D22O4;C6D24O3;	148;162;146;144;	12.5;10.0;34.2;20.0;
168	C7D10O4;C8D20O2;	158;148;	14.7;8.5;
		158;150;162;150;	7.0;49.7;4.9;12.0;
172	C4D14O6;C4D22O5;C6D10O5;C8D22O2;C9D24O;	148;	26.2;
176	C7D14O4;C9D18O2;C9D26O;	162;158;150;	24.5;17.7;57.8;
180	C5D20O5;C6D22O4;	160;158;	81.9;18.1;
184	C5D22O5;C7D26O3;	162;158;	27.7;72.3;
188	C5D16O6;C6D26O4;	172;162;	73.7;26.3;
192	C6D20O5;C10D20O2;	172;172;	93.3;6.7;
196	C4D10O8;C11D24O;	186;172;	45.0;55.0;
200	C8D28O3;	172;	
204	C10D18O3;	186;	

212 C4D10O9;C4D26O7;C8D10O6;C12D26O; 202;186;202;186; 11.1;26.1;52.6;10.1;  
216 C9D14O5; 202;

a) “fundamental” fragments: every other mass can be expressed as a sum of the masses of these fragments, as exemplified in Figure 21S.

**Table 2S.**

Structural attribution of mass loss fragments in ESI MS spectra of EC-*d*<sub>4</sub> in MeCN/D<sub>2</sub>O (assuming single fragment elimination).

mass (D) a.m.u.	mass (H) a.m.u.	shift in H <sub>2</sub> O	relative weight, %	candidate formula	isobar fraction %	tentative neutral fragment identity (w/o isomers)
20	18	1,2	3.86	D2O	100.0	water
32	30	0	22.78	CD2O	83.1	formaldehyde
32	28	0	22.78	C2D4	16.9	ethylene
36	32	1	0.31	CD4O	100.0	methanol
44	44	0	8.97	CO2	100.0	CO2
48	44	1	6.81	C2D4O	100.0	acetaldehyde
52	46	1,2	1.51	C2D6O	34.3	ethanol
52	44	-	1.51	C3D8	65.7	propane
60	58	0	0.7	C2D2O2	88.1	glyoxal
64	62	0,1,2	8.31	CD2O3	25.9	a
64	60	1,2?	8.31	C2D4O2	55.7	glycolaldehyde
64	58		8.31	C3D6O	18.5	EtCHO
68	62	1,2	1.86	C2D6O2	13.1	glycol
68	60	1?	1.86	C3D8O	79.1	propanol
68	58		1.86	C4D10	7.8	butane
76	74	0	3.6	C2D2O3	63.4	formic anhydride
76	72		3.6	C3D4O2	36.6	a
80	72	0,1	3.37	D8O4	40.1	a
80	70	0	3.37	C5D10	59.9	pentene
84	76	1,2	0.67	C3D8O2	54.1	propanediol
84	74	1	0.67	C4D10O	23.6	butanol
84	72		0.67	C5D12	22.4	pentane
88	76	0	0.33	C4D12O	100.0	b
92	88	0,1	3.65	C3D4O3	63.6	ethylene carbonate
92	86		3.65	C4D6O2	36.4	diacetyl, succinaldehyde?
96	92	0,1,2	3.9	C2D4O4	14.3	b
96	90		3.9	C3D6O3	37.0	b
96	88		3.9	C4D8O2	48.8	b
100	90	1,2	0.99	C4D10O2	66.9	butanediol
100	88		0.99	C5D12O	28.6	b
104	102	0	0.37	C3D2O4	100.0	b
108	106	0,1	3.18	C2D2O5	54.7	b
108	104		3.18	C3D4O4	21.2	malonic, hydroxypurinic acids?
108	102		3.18	C4D6O3	16.1	propylene carbonate?
108	100		3.18	C5D8O2	8.0	b

112	100		3.11	C2D12O4	39.9	b
112	106	1,2	3.11	C3D6O4	29.0	glyceric acid, 2-hydroxyethyl H carbonate
112	102	1,2	3.11	C5D10O2	19.6	HO(CH2)4CHO
116	106	1,2	0.43	C4D10O3	58.0	diethylene glycol
116	104	1,2	0.43	C5D12O2	12.6	pentanediol
116	102	1	0.43	C6D14O	29.3	hexanol
120	118	0	0.74	C3D2O5	82.6	b
120	116		0.74	C4D4O4	17.4	b
124	114	0,1,2 w	2.59	C2D10O5	8.6	b
124	120		2.59	C3D4O5	45.1	tartronic acid?
124	118	1,2	2.59	C4D6O4	5.5	succinic acid
124	116		2.59	C5D8O3	23.8	antithermin?
124	114	0	2.59	C6D10O2	17.0	hexanedione (2-hydroxyethoxy)acetic acid? 1,4-dioxane-2,5-diol?
128	120	0,1,2	1.57	C4D8O4	6.4	ethyl carbonate
128	118	1,2	1.57	C5D10O3	22.5	hexanoic acid
128	116	0	1.57	C6D12O2	60.4	heptanal
132	132	0,1,2	0.25	C3O6	39.3	b
132	116		0.25	C3D16O4	15.0	b
132	116		0.25	C7D16O	42.8	heptanol
136	132	0,1,2	0.86	C4D4O5	73.8	oxaloacetic acid
136	130		0.86	C5D6O4	26.2	dioxopentanoic acid?
140	130	0,1,2 w	2.43	C2D10O6	14.1	b
140	132	0	2.43	C5D8O4	85.9	EO-EC, glutaric acid
144	132	0	0.95	C6D12O3	38.7	(EC)3
144	130	1,2	0.95	C7D14O2	46.8	HO(CH2)6CHO?
148	134		0.13	C6D14O3	31.4	diglyme
148	130		0.13	C8D18O	30.4	b
148	128	0	0.13	C9D20	29.1	nonane
152	132	0,1	0.81	C4D20O4	11.0	b
156	146	0,1	1.35	C2D10O7	12.2	b
156	144		1.35	C3D12O6	20.3	b
156	150		1.35	C4D6O6	9.8	b
156	142		1.35	C4D14O5	12.8	b
156	146		1.35	C6D10O4	24.0	adipic acid
156	144		1.35	C7D12O3	8.9	oxoheptanoic acid?
156	142		1.35	C8D14O2	12.0	octanedione
160	146	0,1,2	0.43	C3D14O6	17.2	b
160	148		0.43	C6D12O4	29.9	Ac- or -CH2CO terminated (EO)2H
160	142		0.43	C9D18O	45.8	nonanal
164	150	0	0.21	C2D14O7	17.7	b

164	144		0.21	C5D20O4	82.3	*
168	150	0,1	0.89	C3D18O6	63.5	*
168	148		0.89	C4D20O5	33.9	*
172	158	0,1,2	0.88	C4D14O6	69.6	*
172	162		0.88	C6D10O5	30.4	*
176	160		0.23	C4D16O6	48.5	*
176	158	2	0.23	C5D18O5	46.2	*
180	162	0	0.17	D18O9	100.0	*
184	172	1	0.57	C4D12O7	100.0	MeO(O)C(CO)2(CHOH)2CH2OH?
188	174	0,1,2	0.33	C8D14O4	18.4	HOOC(CH2)6COOH?
188	172		0.33	C9D16O3	81.6	HCO(CH2)7COOH?
192	172	0	0.1	C2D20O8	59.0	*
192	174		0.1	C5D18O6	6.2	*
192	174		0.1	C9D18O3	16.4	HO(CH2)8COOH?
192	172		0.1	C10D20O2	18.4	C5- (EO)2H
196	186	0,1	0.29	C4D10O8	62.0	*
196	188		0.29	C7D8O6	8.9	*
196	176		0.29	C9D20O3	29.1	*
200	186	0,1	0.33	C9D14O4	100.0	*
204	188		0.15	C5D16O7	80.3	*
204	192		0.15	C7D12O6	19.7	*
212	202		0.12	C4D10O9	100.0	*
216	202		0.13	C9D14O5	100.0	HOOC(CH2)3CO(CH2)3COOH?

- a) composite (loss of two or more fragments)  
 b) no match in ChemSpider structural database.

**Table 3S.**

Summary of  $^{19}\text{F}$  and  $^{31}\text{P}$  NMR peaks observed in irradiated solution of EC containing 1 M Li PF<sub>6</sub>

$^{19}\text{F}$ shift, ppm vs. CFCl <sub>3</sub>	coupling pattern	J( $^{31}\text{P}$ - $^{19}\text{F}$ ), Hz	$^{31}\text{P}$ shift, ppm, vs. $\text{H}_3\text{PO}_4$	coupling pattern	species
-71.01	<i>d</i>	711.14	-144.22	<i>septet</i>	PF <sub>6</sub> <sup>-</sup>
-78.62	<i>d</i>	949.6	-16.05	<i>t</i>	PF <sub>2</sub> O <sub>2</sub> <sup>-</sup>
-149.7	<i>d</i>	1134	(-1 to -5)	<i>d?</i>	PFO <sub>3</sub> <sup>2-</sup>

**Table 4S.**

<sup>1</sup>H-<sup>1</sup>H COSY cross peaks observed in irradiated EC (1.83 MGy) in DMSO-*d*<sub>6</sub>.

$\delta(^1\text{H})$ , ppm vs. TMS	coupling pattern	$J(^1\text{H}-^1\text{H})$ , Hz	cross peaks at $\delta(^1\text{H})$ , ppm vs. TMS			
9.67	<i>q</i>	2.8		2.136		
9.55	<i>s</i>			6.235		
8.21	<i>d</i>	6.2		4.11		
7.13	<i>s</i>			4.265		
6.6	<i>t</i>	5.4		4.36	4.6	5.28
6.42	<i>t</i>	9.5		4.66		
6.25	<i>td?</i>	7.9, 7.8		4.63		
6.17	<i>s</i>			4.62		
5.86	<i>ddd</i>	10.7, 5.5, 2.7		4.62		
5.375	<i>dd</i>	9.1, 5.2		4.71		
5.297	<i>dd</i>	9.5, 5.6		4.646		
5.247	<i>t</i>	5.5		3.503	3.677	4.086
5.13	<i>tt</i>	2.7, 6.8		4.42		5.282
5.12	<i>s</i>			4.615		
5.07	<i>ddt</i>	8.0, 5.3, 0.9		4.44		
4.9	<i>m</i>			1.406		
4.855	<i>q</i>	4.9		1.247		
4.783	<i>m</i>			3.534		
4.777	<i>ddt</i>	8.7, 5.8, 3.0		4.329	4.44	
4.766	<i>s</i>			3.677		
4.622	<i>s</i>			5.075		
4.611	<i>s</i>			1.12		
4.583	<i>t</i>	8.0?		4.174		
4.169	<i>t</i>	7.9		4.583		
4.086	<i>t</i>	4.8		3.582		
3.864	<i>t?</i>	7.1		3.445		
3.86	<i>t?</i>	7.1		5.47		
3.737	<i>s</i>			3.884		
3.665	<i>t?</i>	18.6?		3.518	5.282	1.29
3.56	<i>s</i>			4.09		
3.505	<i>ddd</i>	9.8, 5.7, 2.8		3.661	5.25	
3.48	<i>q</i>	7		1.09		
3.422	<i>q</i>	6.9		4.33		
3.37	<i>s</i>			4.39		
3.282	<i>s</i>			9.06		
3.15	<i>s</i>			4.075		
2.62	<i>s</i>			3.68		
2.586				9.396	9.539	9.635
2.57	<i>s</i>			3.71		4.503
2.497	<i>s</i>			3.645		
2.42	<i>s</i>			3.65		
2.38	<i>s</i>			0.93		
2.348	<i>t</i>	6.3		3.614		

<b>2.105</b>	<i>d</i>	3	9.67
<b>2.033</b>	<i>s</i>		4.408
<b>2.011</b>	<i>s</i>		4.043
<b>1.95</b>	<i>s</i>		3.55
<b>1.9</b>	<i>s</i>		4.503
<b>1.878</b>	<i>s</i>		3.566
<b>1.845</b>	<i>s</i>		3.518
<b>1.822</b>	<i>s</i>		1.326 3.947 3.53
<b>1.684</b>	<i>dd or qq</i>	7.4, 6.3	0.897
<b>1.219</b>	<i>dd</i>	4.9, 1.3	4.87
<b>1.13</b>	<i>dd</i>	4.63	4.63
<b>1.109</b>	<i>t</i>	7	3.74
<b>1.053</b>	<i>t</i>	7	3.439
<b>1.02</b>	<i>d</i>	7	3.884
<b>0.904</b>	<i>t</i>	7.4	1.676

**Captions to Figures 1S to 30S.****Figure 1S.**

Estimated chemical shifts ( $\delta(^{13}\text{C})$  in ppm vs. TMS) for carbon-13 nuclei in selected species derived from ethylene carbonate as calculated using B3LYP/6-31+G(d,p) method (in blue) compared to experimentally determined parameters, where available (in purple). The symmetry group of an oligomer molecule is indicated for  $(\text{VC})_n$  species.

**Figure 2S.**

Experimental chemical shifts for carbon-13 nuclei in selected reference species (in  $\text{CDCl}_3$ ); AIST database.

**Figure 3S.**

Proton chemical shifts ( $\delta(^1\text{H})$ , in ppm vs. TMS), for selected species derived from ethylene carbonate, as calculated using B3LYP/6-31+G(d,p) method (in blue) and experimentally determined (in purple).

**Figure 4S.**

Proton chemical shifts ( $\delta(^1\text{H})$ , in ppm vs. TMS) for selected reference species in  $\text{CDCl}_3$ .

**Figure 5S.**

ESI MS<sub>1</sub> spectrum for EC electrosprayed in methanol that was obtained immediately after dispensing of the material from a container obtained from the manufacturer. Two mass-44 progressions, A and B, are indicated.

**Figure 6S.**

Like Figure 5S after one week of solvolysis at room temperature. Several mass-44 progressions are indicated in the plot, and extrapolated onsets of these series are indicated in the legend.

**Figure 7S.**

Normalized ESI MS<sub>2</sub> (neutral fragment loss) spectra for selected mass peaks in Figure 6S. The *m/z*'s for these cations are given at the top of the plot. Mass loss peaks belonging to different mass-44 progressions shown in Figure 6S have somewhat different MS<sub>2</sub> spectra. See the text for more discussion.

**Figure 8S.**

Normalized ESI MS<sub>2</sub> spectra for protonated tetraethylene glycol (*m/z* +195) and pentaethylene glycol (*m/z* +239). The latter was present as impurity in the title compound. The arrows indicate mass-44 shifts. The diagram summarizes fragmentation pathways.

**Figure 9S.**

As Figure 8S, for tetraglyme.

**Figure 10S.**

Variations of ESI MS<sub>2</sub> spectra for  $m/z$  +487 peak in Figure 1 as a function of collisional energy EN (arbitrary units). If not stated otherwise, MS<sub>2</sub> spectra shown in other figures were obtained for EN=25. Within the limitations imposed by counting statistics, the positions of the mass peaks do not change with increasing collisional energy, while ion counts slightly vary with this collisional energy.

**Figure 11S.**

Effect of mass selection window on the ESI MS<sub>2</sub> spectra for  $m/z$  +357 cation (EC radiolysis, 1.8 MGy; electrosprayed in methanol).

**Figure 12S.**

ESI MS<sub>2</sub> spectra for selected cations in the mass spectra of irradiated EC (12.1 MGy) electrosprayed in DMSO/D<sub>2</sub>O. As in protiated solvents, this mass spectrum does not depend on the mass of the parent cation for  $m/z > 300$  a.m.u.

**Figure 13S.**

A comparison of ESI MS<sub>2</sub> spectra obtained for  $m/z$  +357 cation for EC radiolyzate (12.1 MGy) electrosprayed in DMSO containing light and heavy water. This plot reveals the occurrence of facile, multiple H/D exchange in the parent cation.

**Figure 14S.**

ESI MS<sub>1</sub> spectra obtained for radiolyzate generated by low-dose irradiation of EC containing 1 M Li PF<sub>6</sub> (0.85 MGy) and electrosprayed in DMSO/H<sub>2</sub>O (the top panel) and methanol (the bottom panel).

**Figure 15S.**

ESI MS<sub>1</sub> spectra of a water-insoluble residue (see the text) generated in radiolysis of EC solution containing 1 M Li PF<sub>6</sub> (irradiated to 8.5 MGy). Note the logarithmic vertical scale. The material was electrosprayed in an acetonitrile solution.

**Figure 16S.**

ESI MS<sub>2</sub> spectra for specified parent cations from the MS<sub>1</sub> spectrum shown in Figure 15S. The dotted line indicates the MS<sub>2</sub> spectrum of the irradiated EC solution before the treatment aiming to separate the polymer residue.

**Figure 17S.**

ESI MS<sub>2</sub> spectra for selected parent cations in the MS<sub>1</sub> spectra of irradiated EC-*d*<sub>4</sub> (3.6 MGy) electrosprayed in methanol.

**Figure 18S.**

As Figure 17S, for electrospraying of the same radiolyzate in 1:1 v/v acetonitrile-D<sub>2</sub>O.

**Figure 19S.**

Mass-44 intervals observed in the ESI MS<sub>2</sub> spectrum for  $m/z$  +333 parent cation in irradiated EC-*h*<sub>4</sub> that was electrosprayed in acetonitrile-H<sub>2</sub>O solution (Figure 3). The open circles indicate mass loss peaks observed in the cations derived from solvolytically generated (C<sub>2</sub>H<sub>4</sub>X)<sub>n</sub> polymers (Figure 7S).

**Figure 20S.**

As Figure 19S, for EC-*d*<sub>4</sub> in acetonitrile-D<sub>2</sub>O (Figure 3). Mass-44 and mass-48 intervals are indicated by the arrows shown in the plot.

**Figure 21S.**

Genetic algorithm analysis of the mass loss spectrum shown in Figure 3. ESI MS<sub>2</sub> spectrum (i) for EC-*d*<sub>4</sub> in D<sub>2</sub>O serves as the program input. For every fragment peak in this spectrum (with the mass rounded to a whole number), a list of all possible isobaric C<sub>x</sub>D<sub>y</sub>O<sub>z</sub> structures was generated. Then it was tested whether the species can be decomposed into the several “fundamental” fragments with the masses and structures given in the Table 1S (this process is illustrated for mass-124 fragment). The isobars in the short list were given equal weights and spectrum (i) was mapped on the ESI MS<sub>2</sub> spectrum (iii) for irradiated EC-*h*<sub>4</sub> in H<sub>2</sub>O (also from Figure 3), giving each isobar -y mass shift (trace (ii)). These weights were optimized to obtain the minimal rms deviation between traces (ii) and (iii). The isobars with the relative weights < 5% were eliminated and the optimization was performed once again. The resulting histograms (like the one shown at the top) gives relative abundances of the selected isobars for each fragment peak in trace (i). The results of this analysis are given in Table 1S and Figure 22S.

**Figure 22S.**

Genetic algorithm analysis of trace (i) in Figure 21S. Chemical formulae in Table 1S were screened using the ChemSpider structural database by the Royal Society of Chemistry, assuming, where possible, single fragment progenitors (see also Table 2S). Only one isomer is given for homologous compounds.

**Figure 23-24S (in two panels).**

<sup>13</sup>C NMR spectra (obtained in DMSO-*d*<sub>6</sub>) for (i) EC before irradiation, (ii) irradiated EC (2 MGy), and (iii, iv) solution containing 1 M Li PF<sub>6</sub> that was irradiated to 8.5 MGy. Solution (iv) was 10x more concentrated than solution (iii). Off-scale resonances of methylene and carbonyl carbons in the parent compound are not shown.

**Figure 25-30S (in six panels).**

<sup>1</sup>H NMR spectra (obtained in DMSO-*d*<sub>6</sub>) for (i) EC before irradiation, and EC solution irradiated to the total dose of (ii) 1.8 and (iii) 12 MGy. J(<sup>1</sup>H-<sup>1</sup>H) couplings in Hz are given in the parentheses, and chemical shifts for cross peaks in <sup>1</sup>H-<sup>1</sup>H COSY spectra are given following the “::” separator.

**Figure 1S, Shkrob et al.**

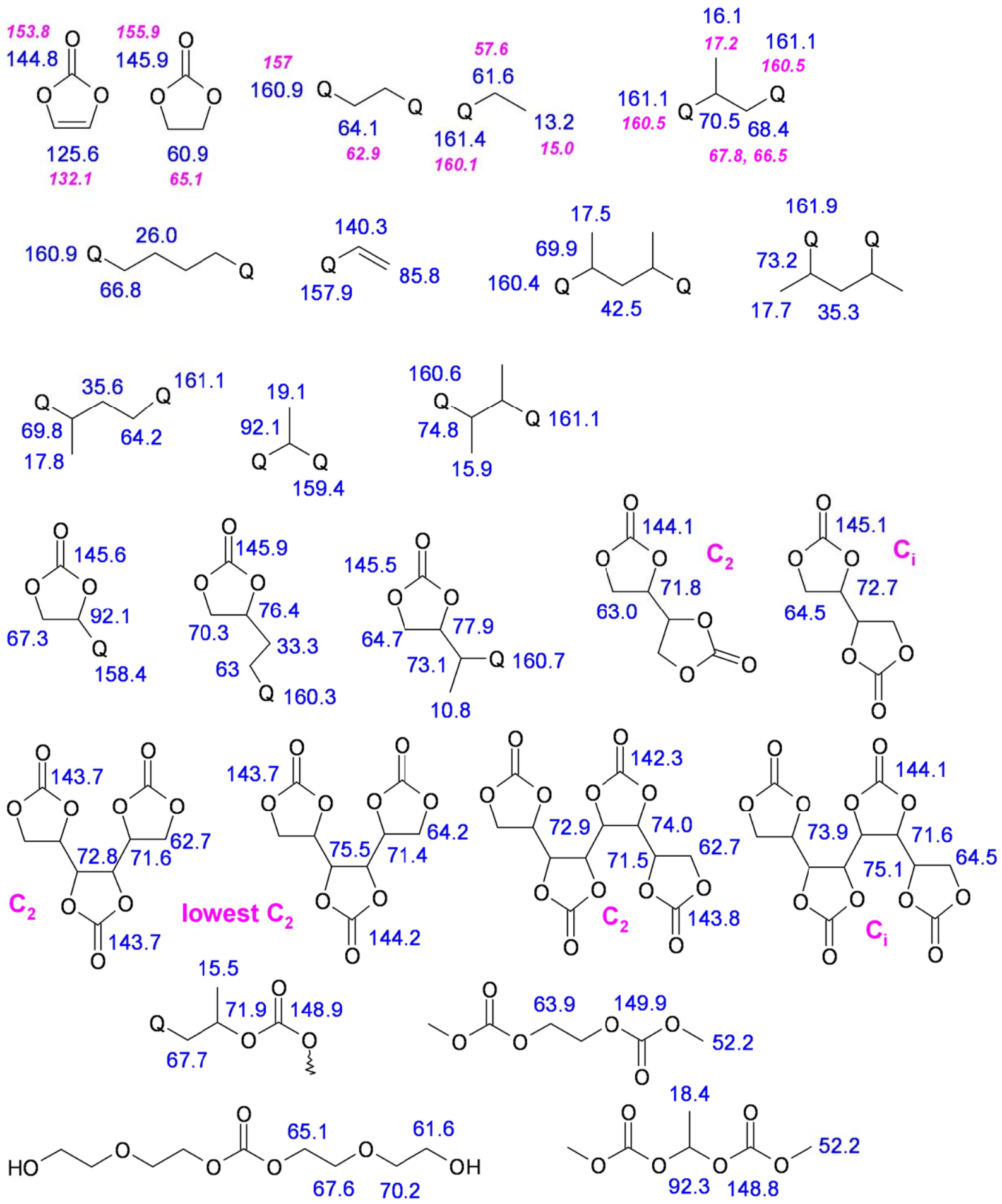


**Figure 2S, Shkrob et al.**

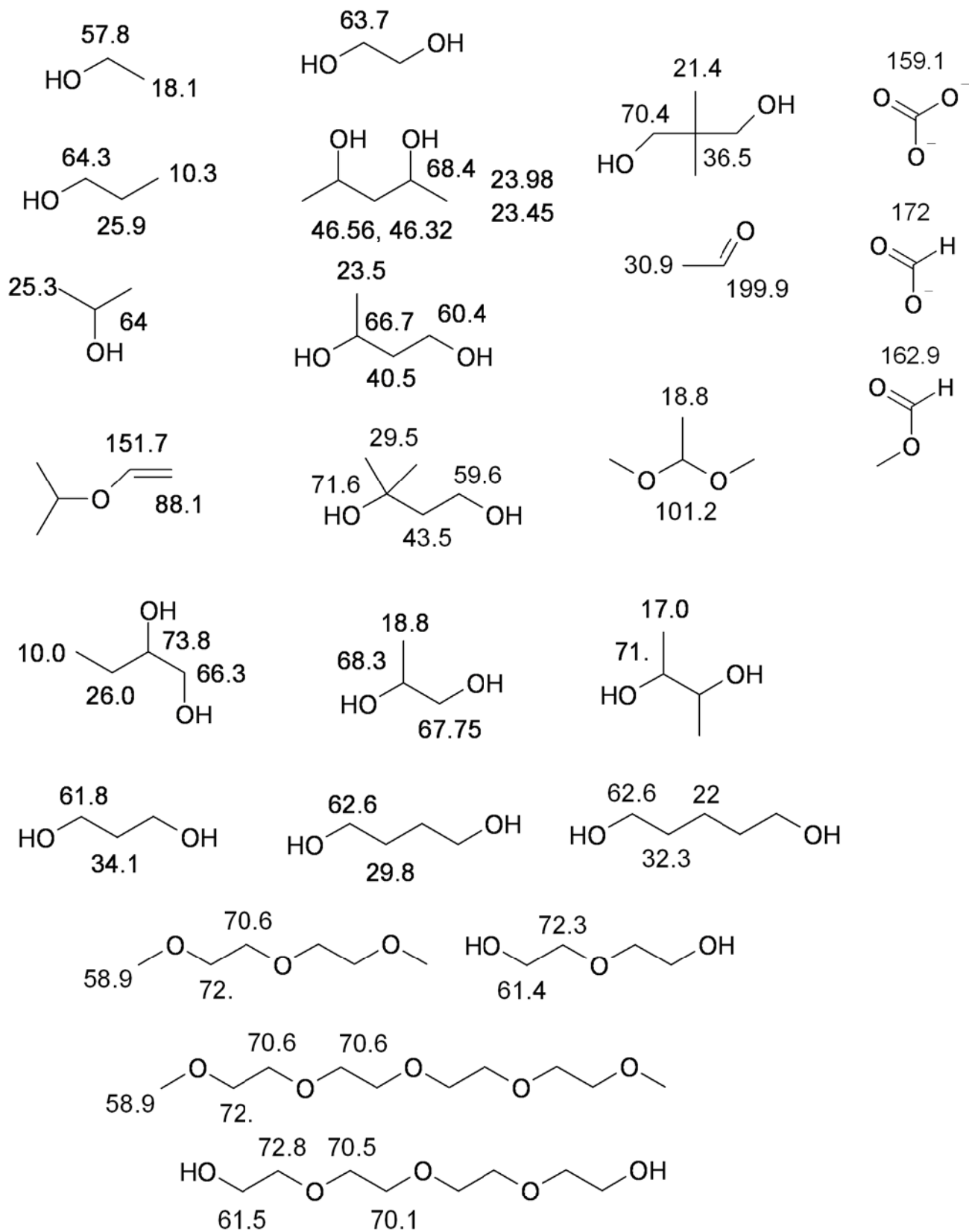


**Figure 3S, Shkrob et al.**

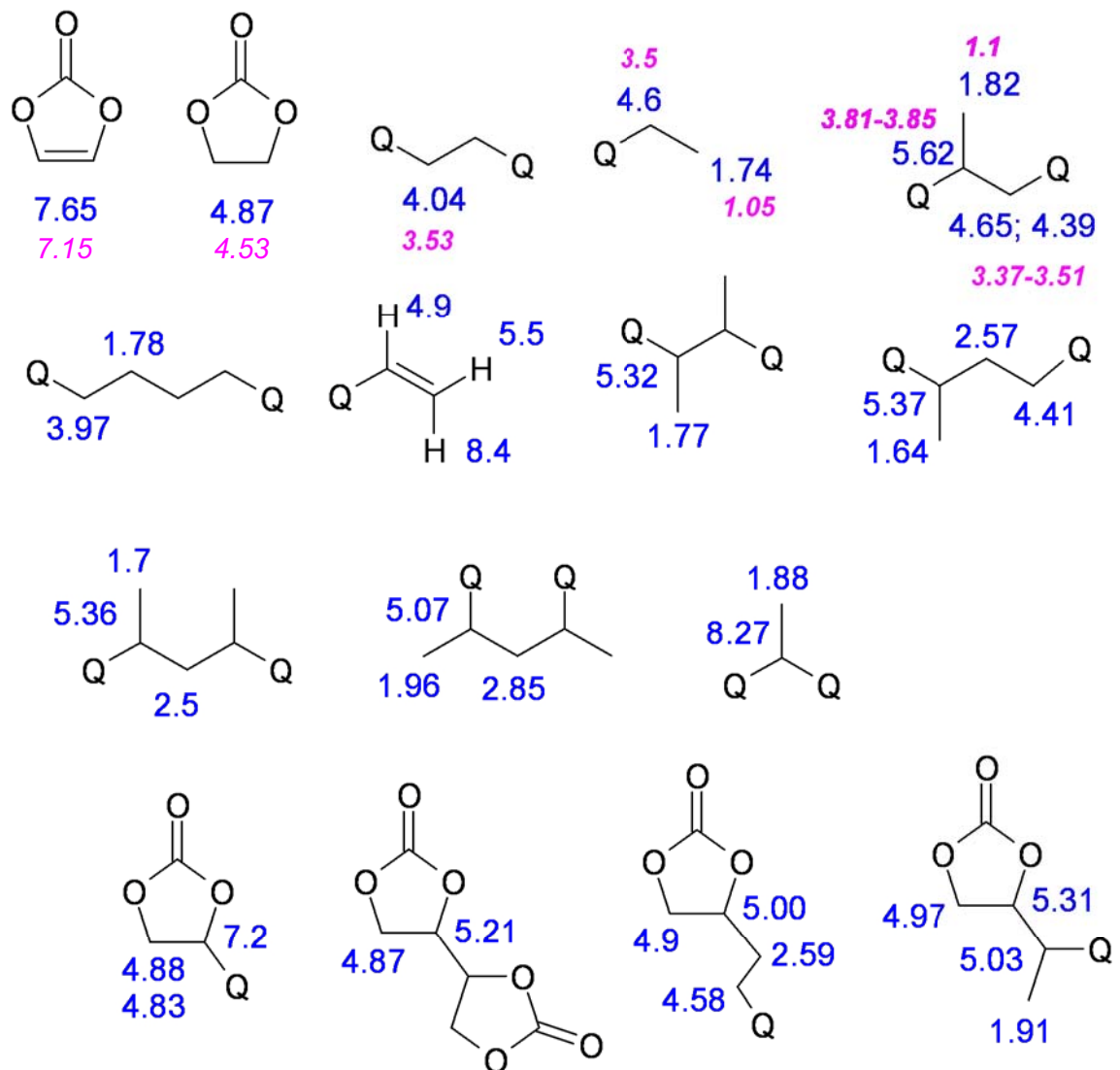


**Figure 4S, Shkrob et al.**

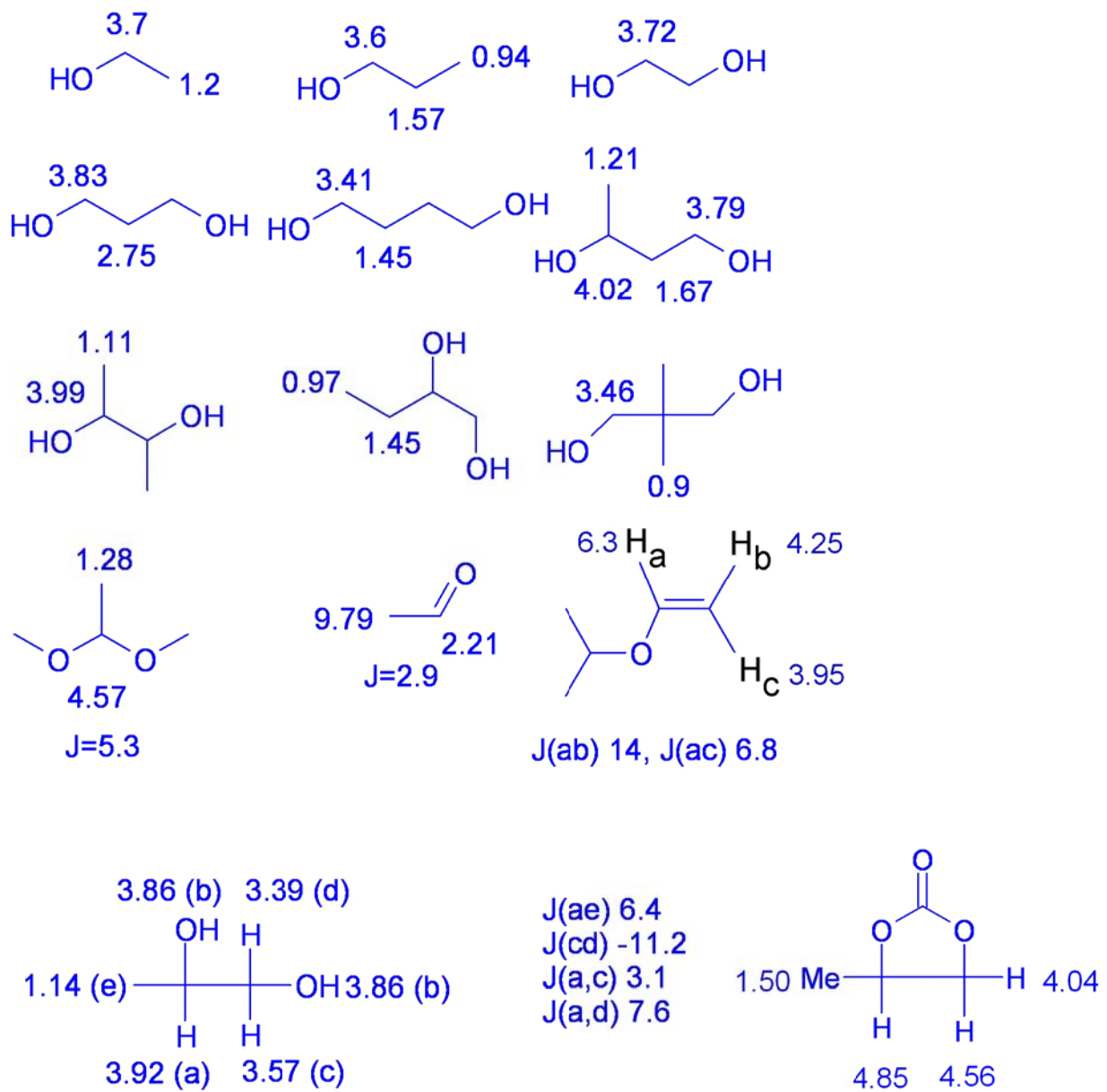


**Figure 5S, Shkrob et al.**

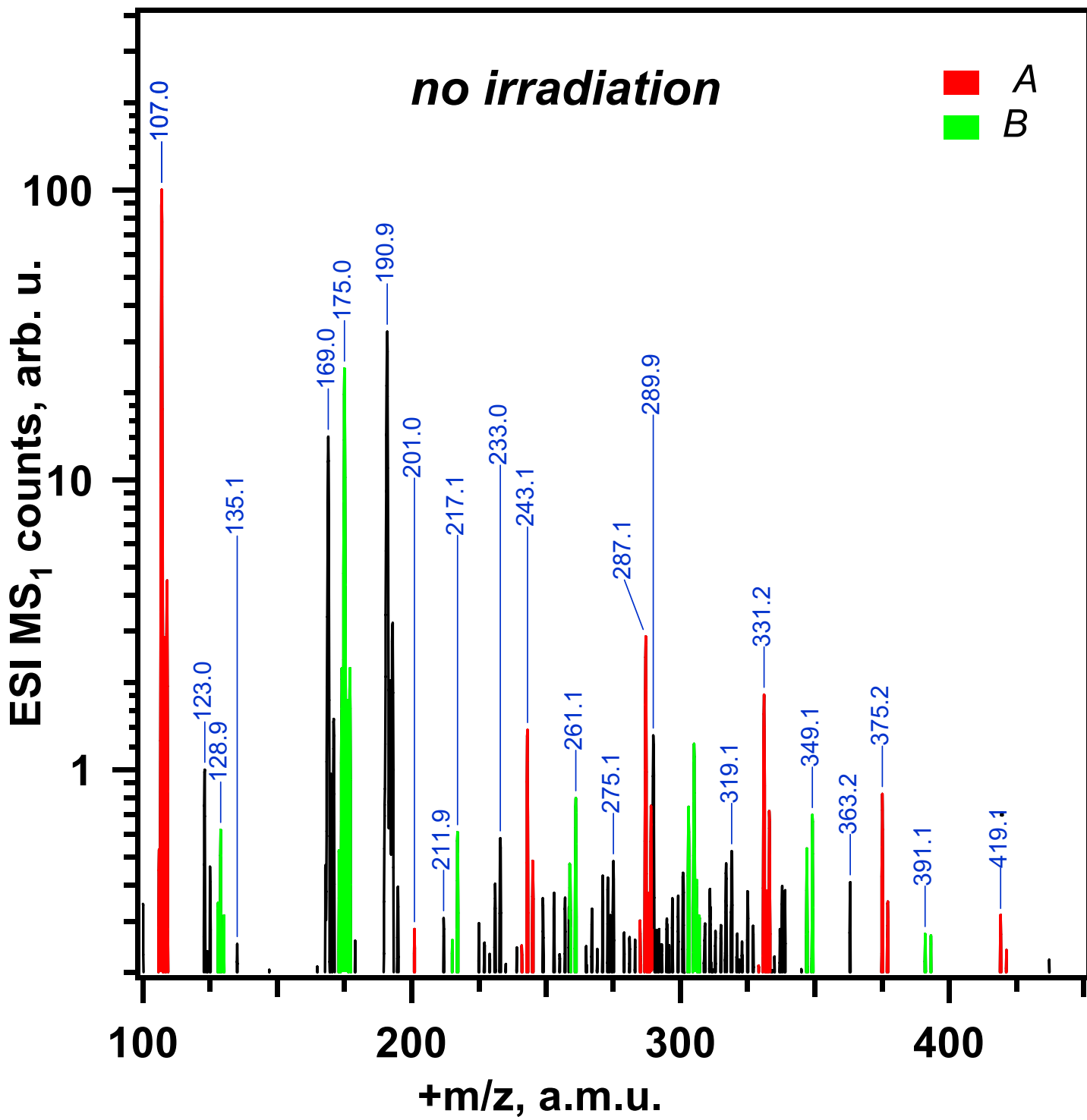
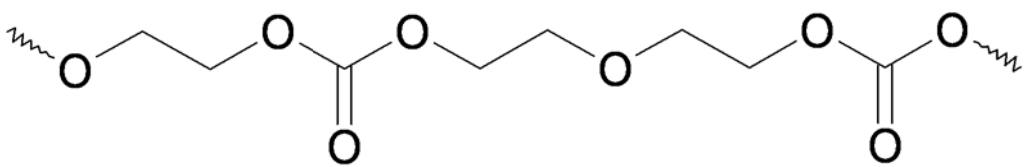
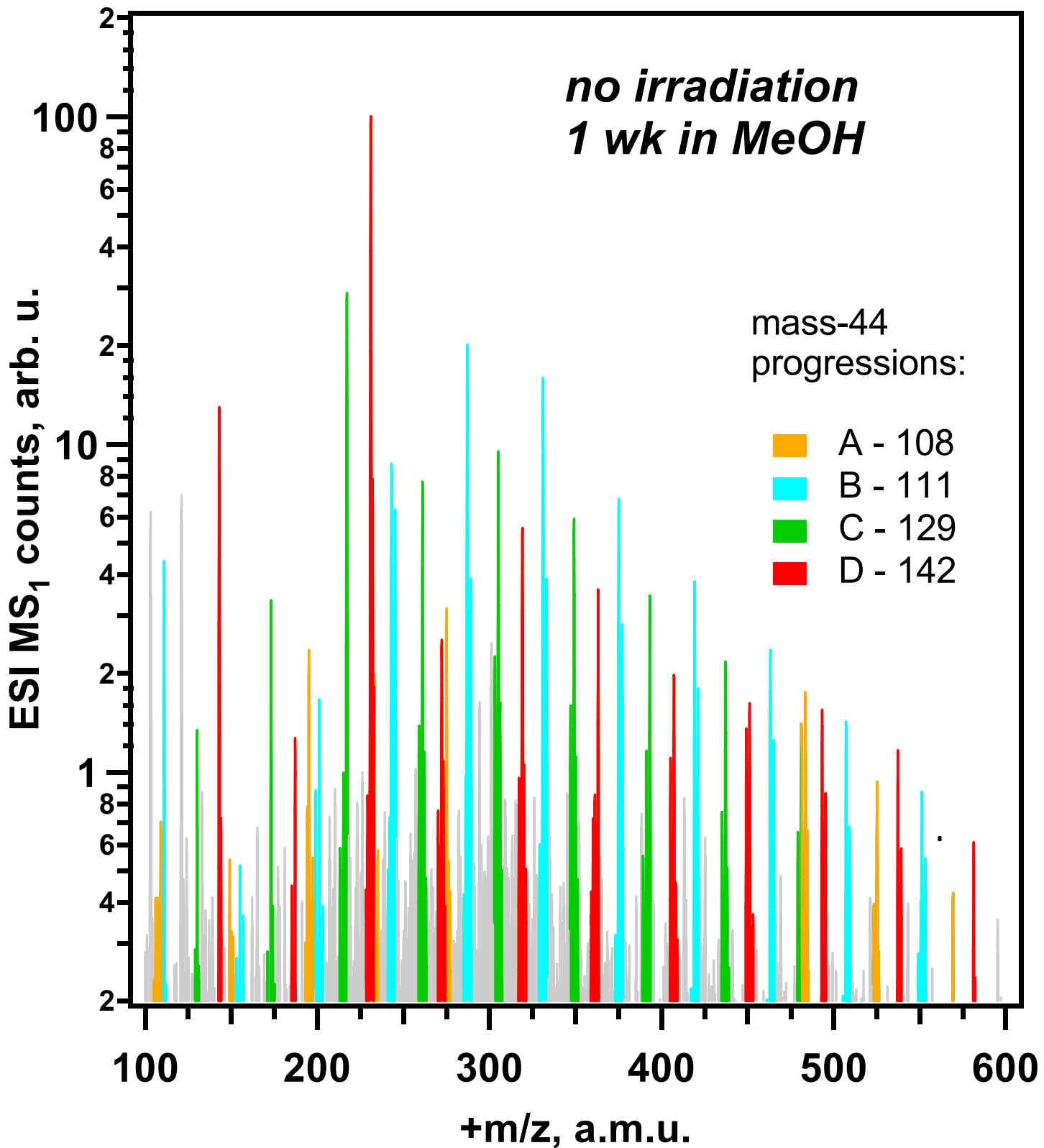
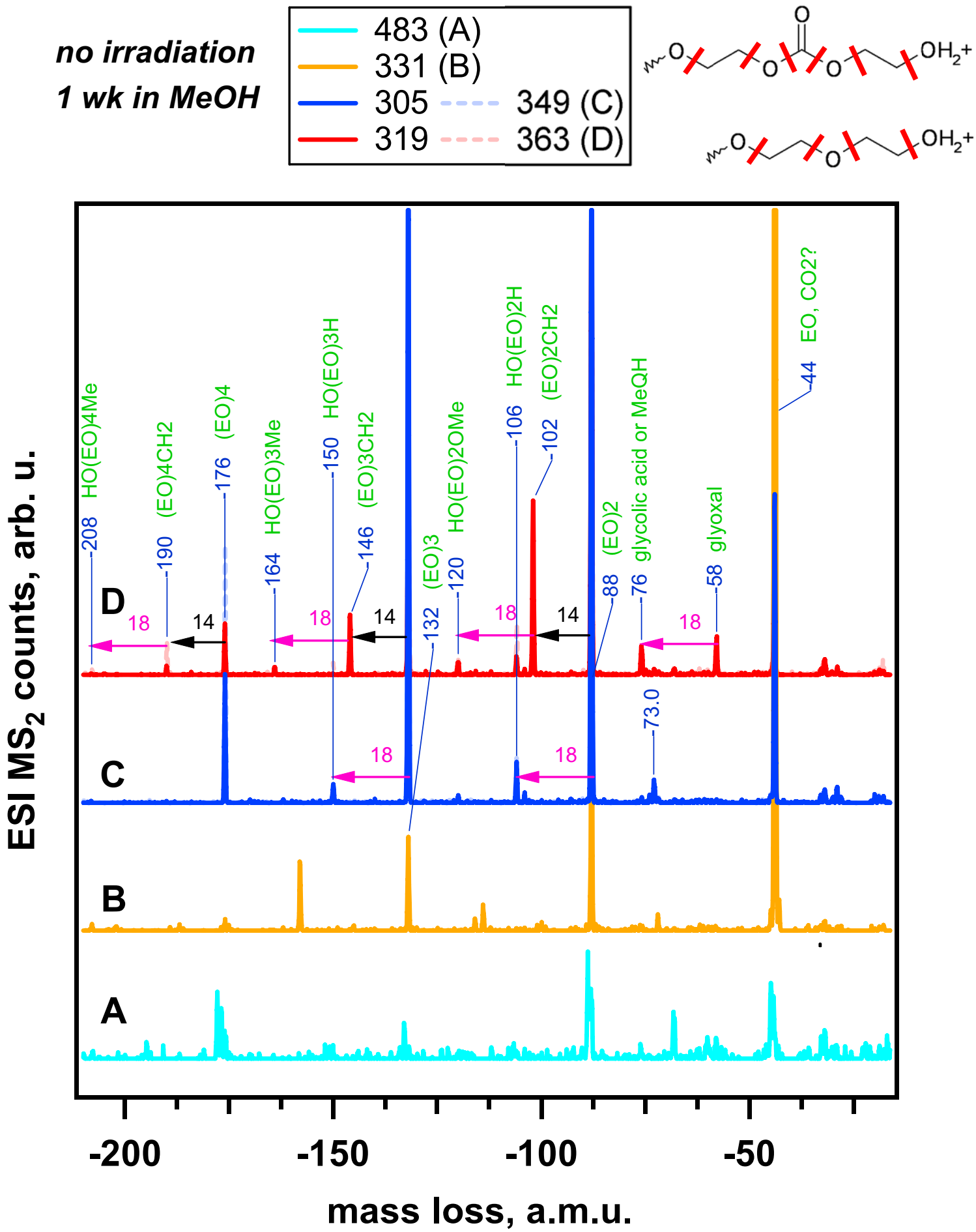


Figure 6S, Shkrob et al.



**Figure 7S, Shkrob et al.**



**Figure 8S, Shkrob et al.**

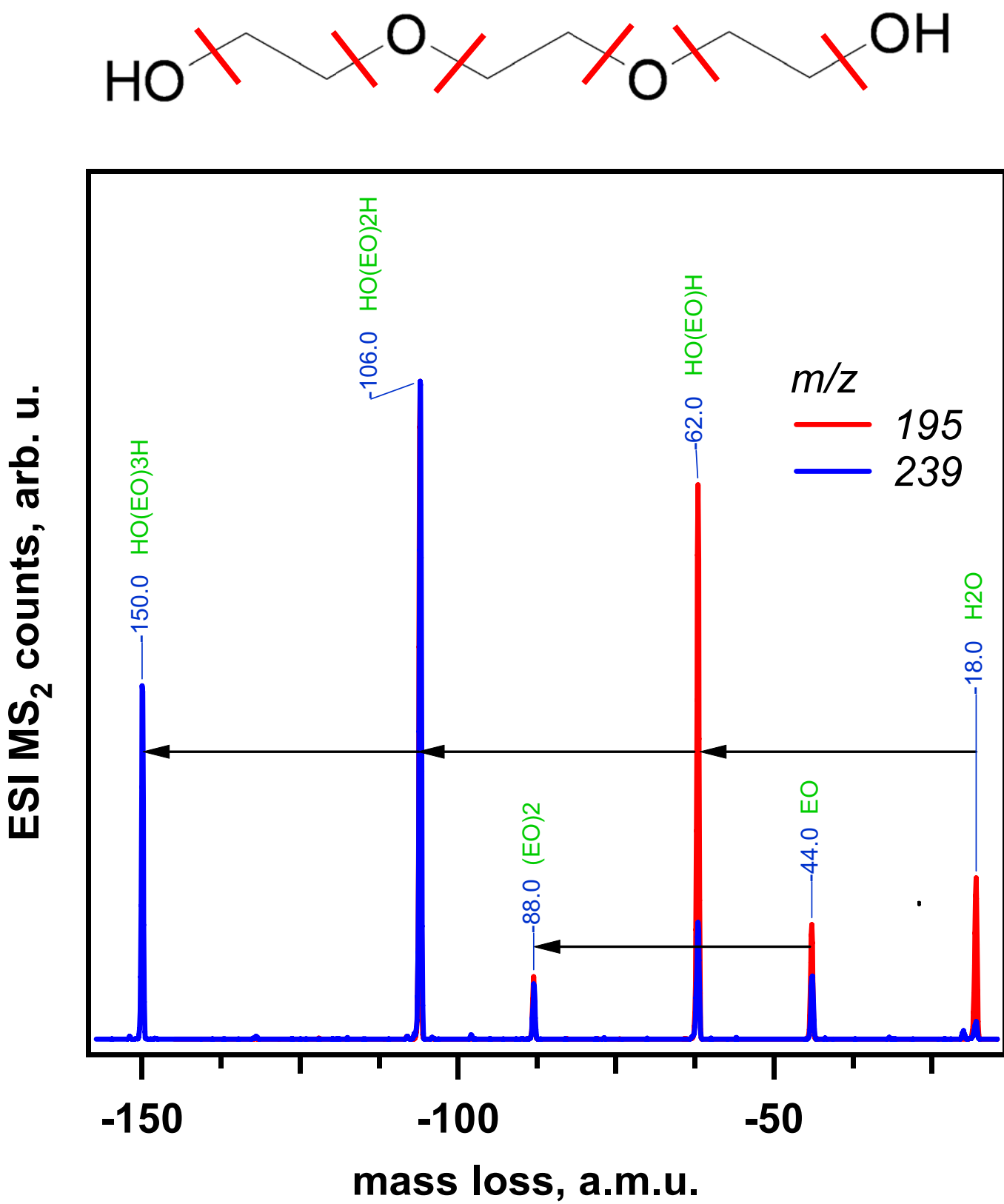


**Figure 9S, Shkrob et al.**

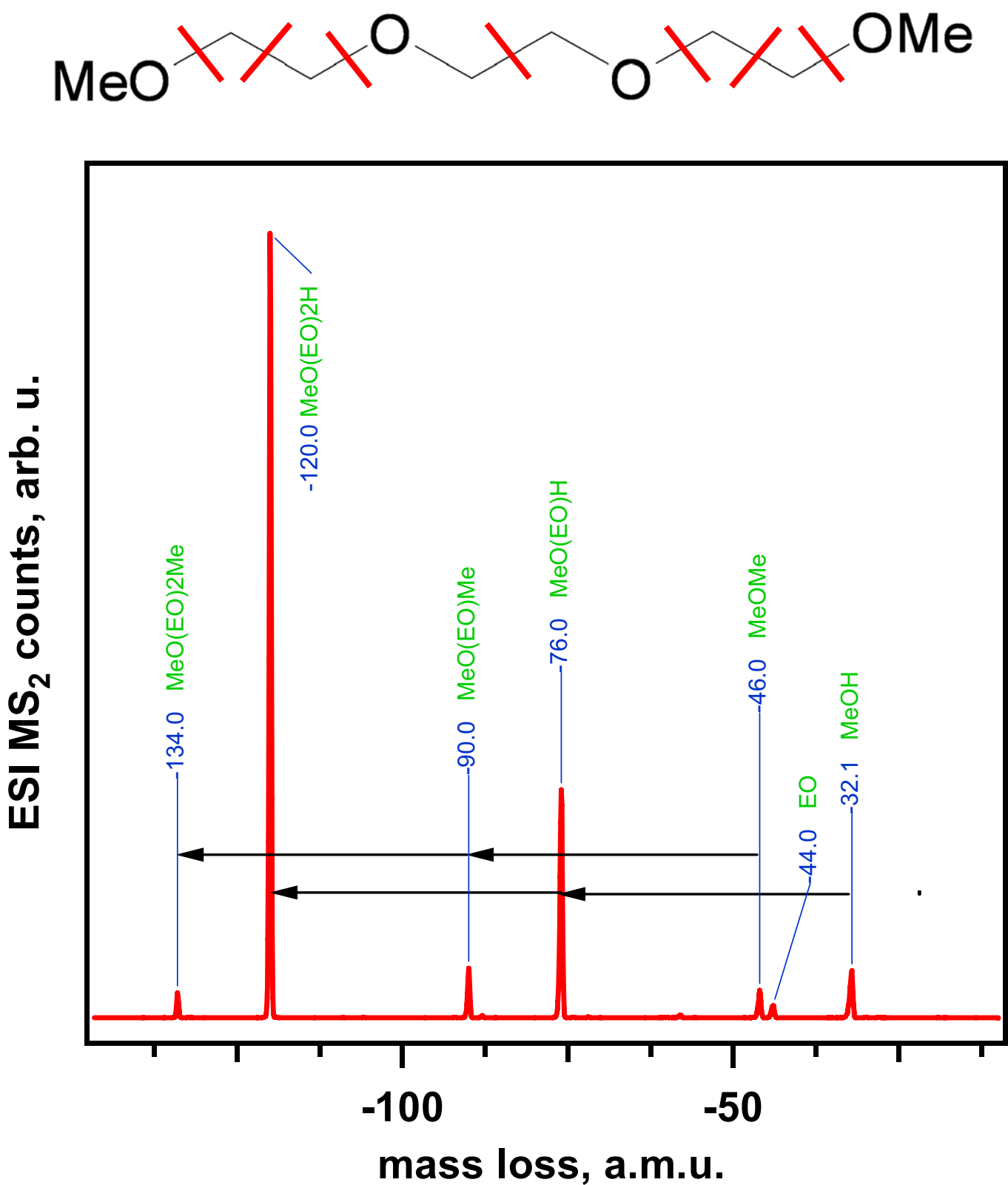


**Figure 10S, Shkrob et al.**

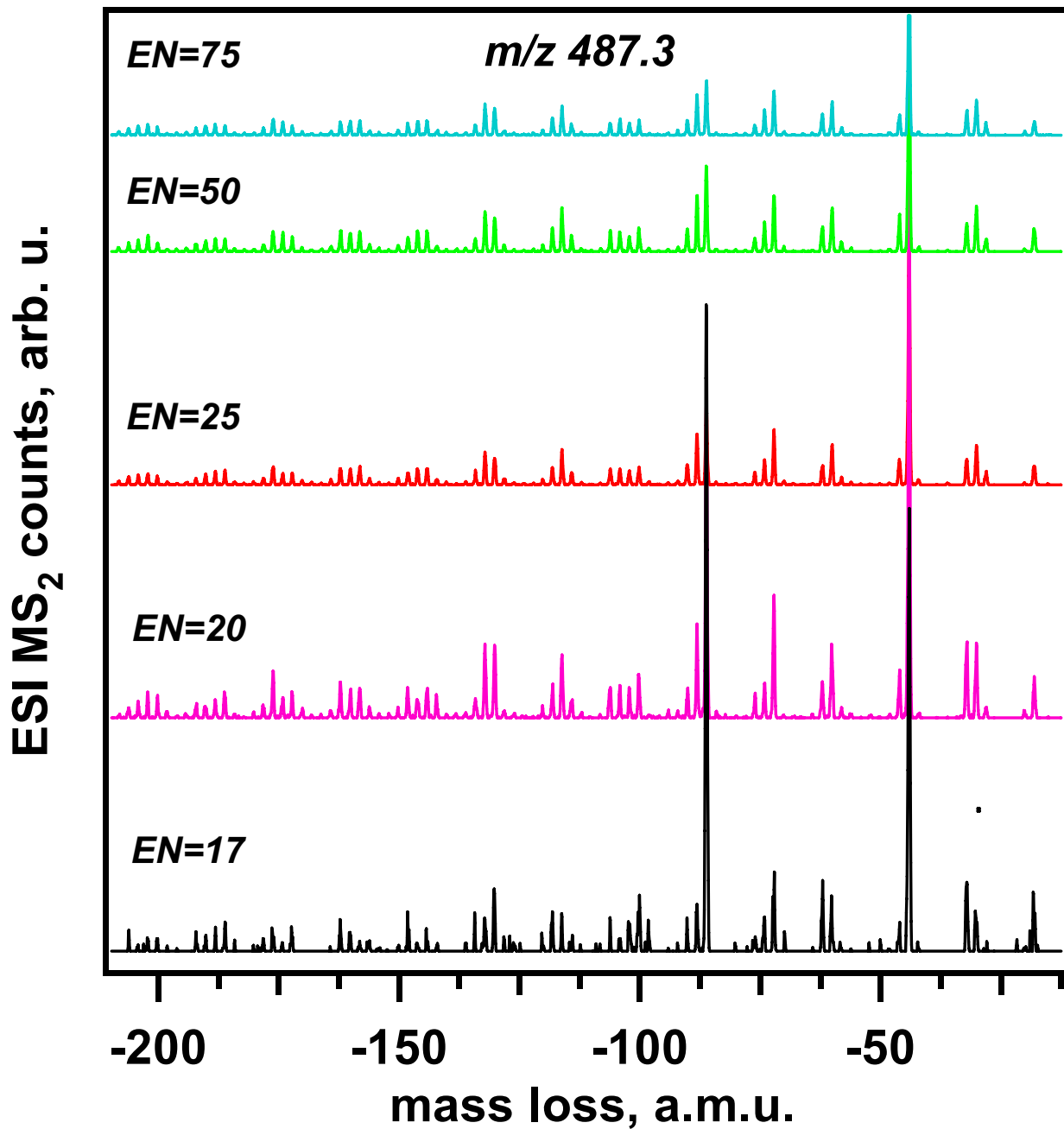


**Figure 11S, Shkrob et al.**

ESI MS<sub>2</sub> counts, arb. u.

*low dose radiolysis  
of EC (1.83 MGy)*

*m/z=+357.2  
mass selection,  
a.m.u*

— 2.0  
— 1.0  
— 0.5

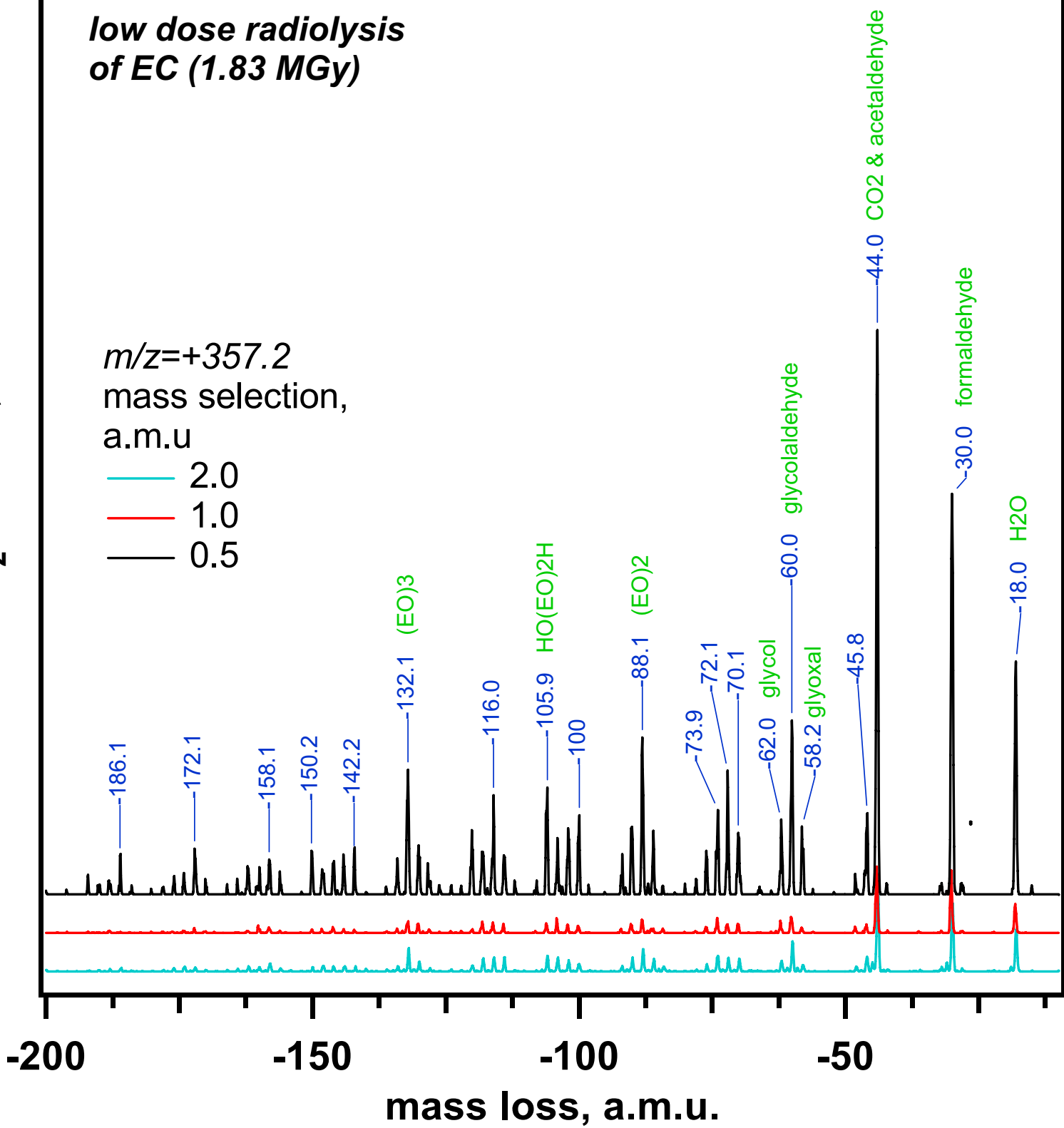


**Figure 12S, Shkrob et al.**

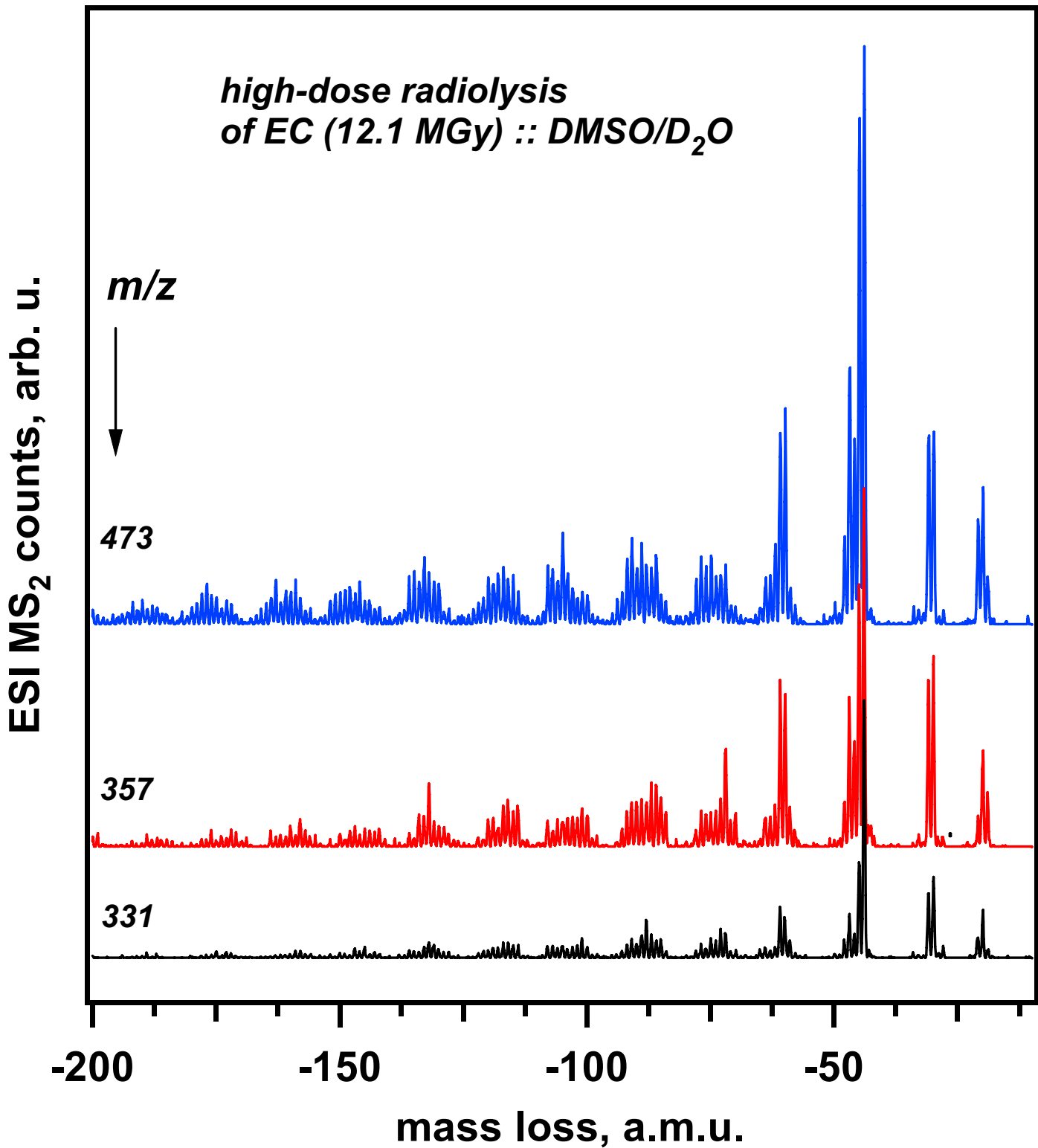
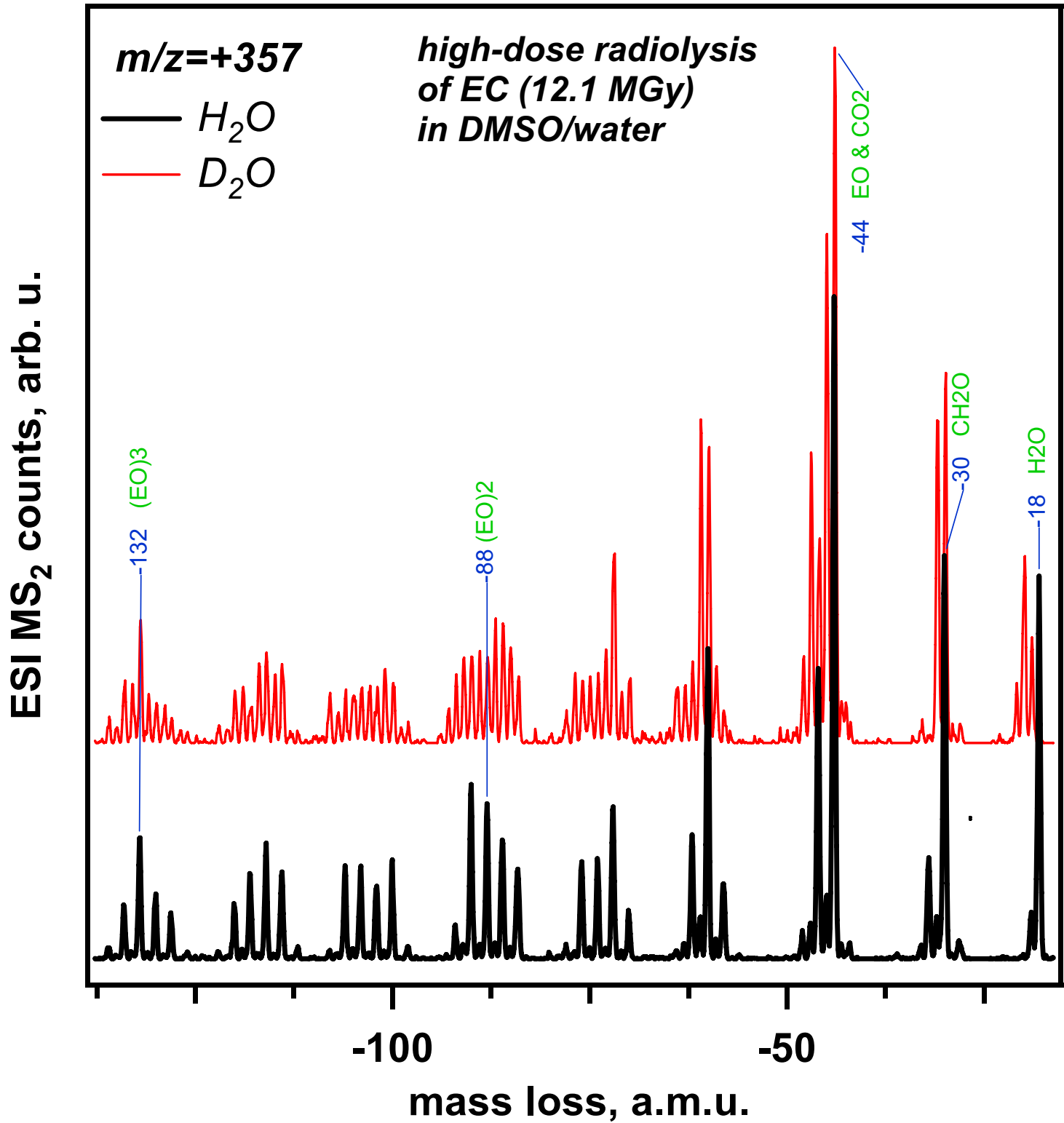
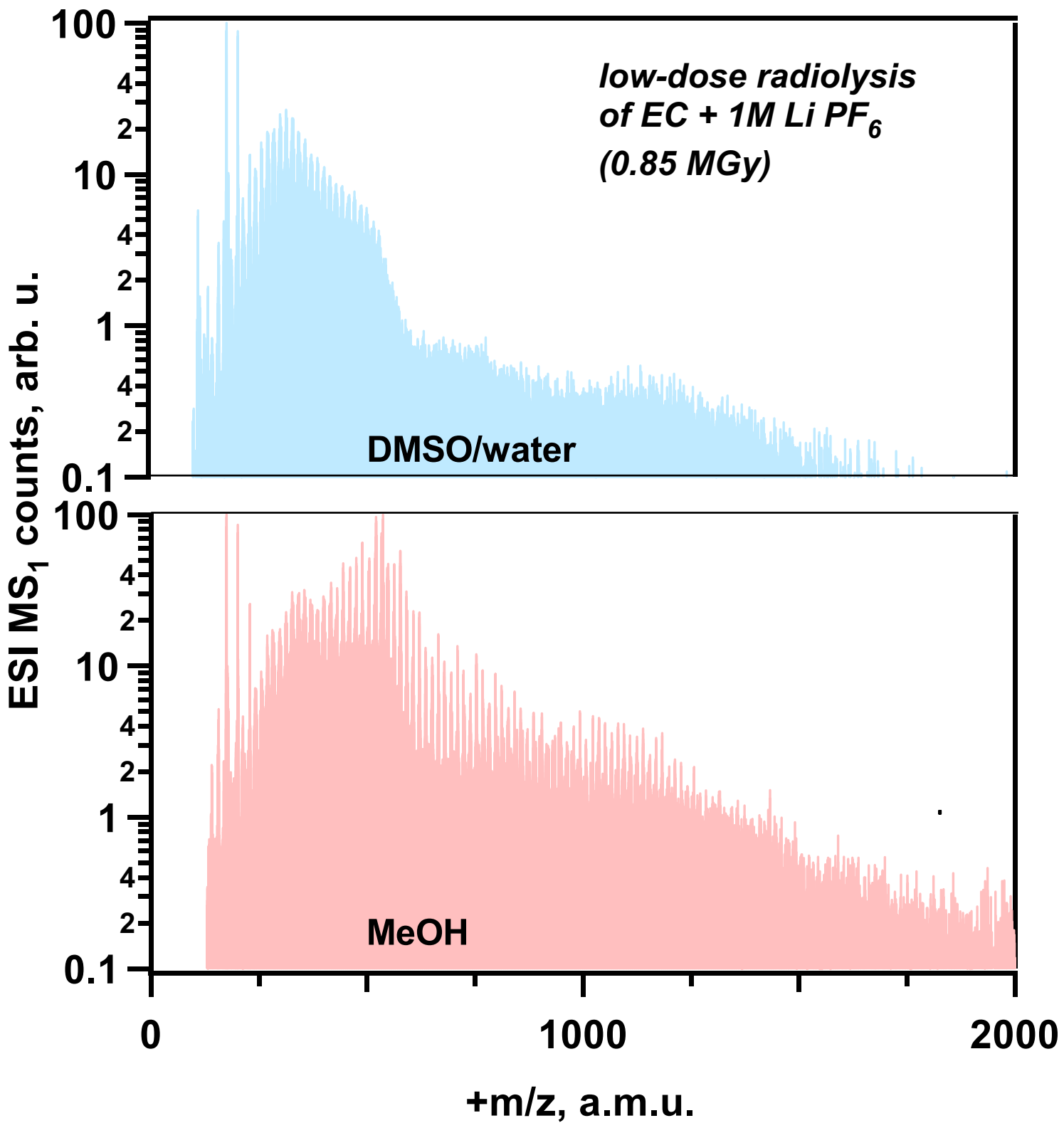


Figure 13S, Shkrob et al.



**Figure 14S, Shkrob et al.**



**Figure 15S, Shkrob et al.**

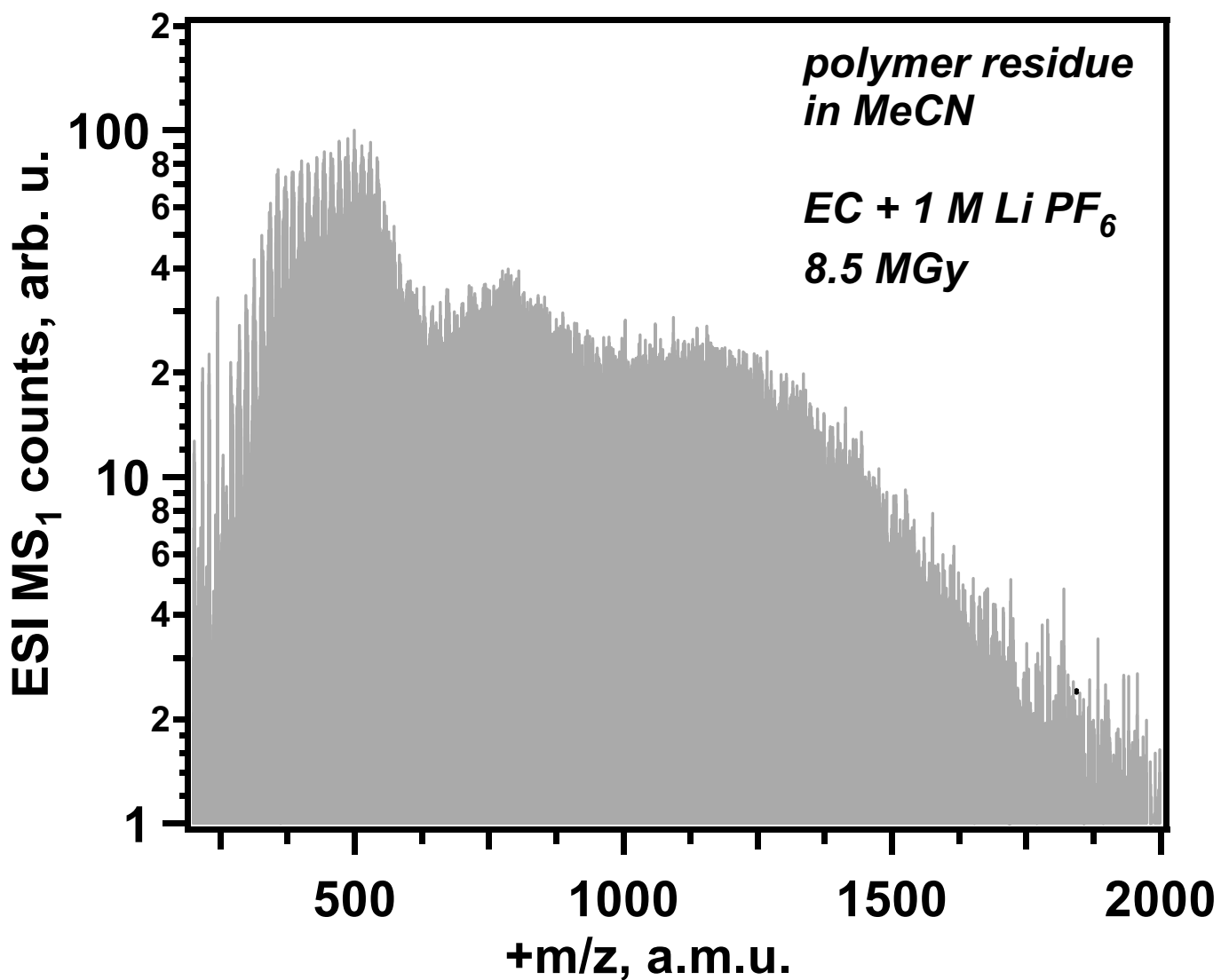


**Figure 16S, Shkrob et al.**

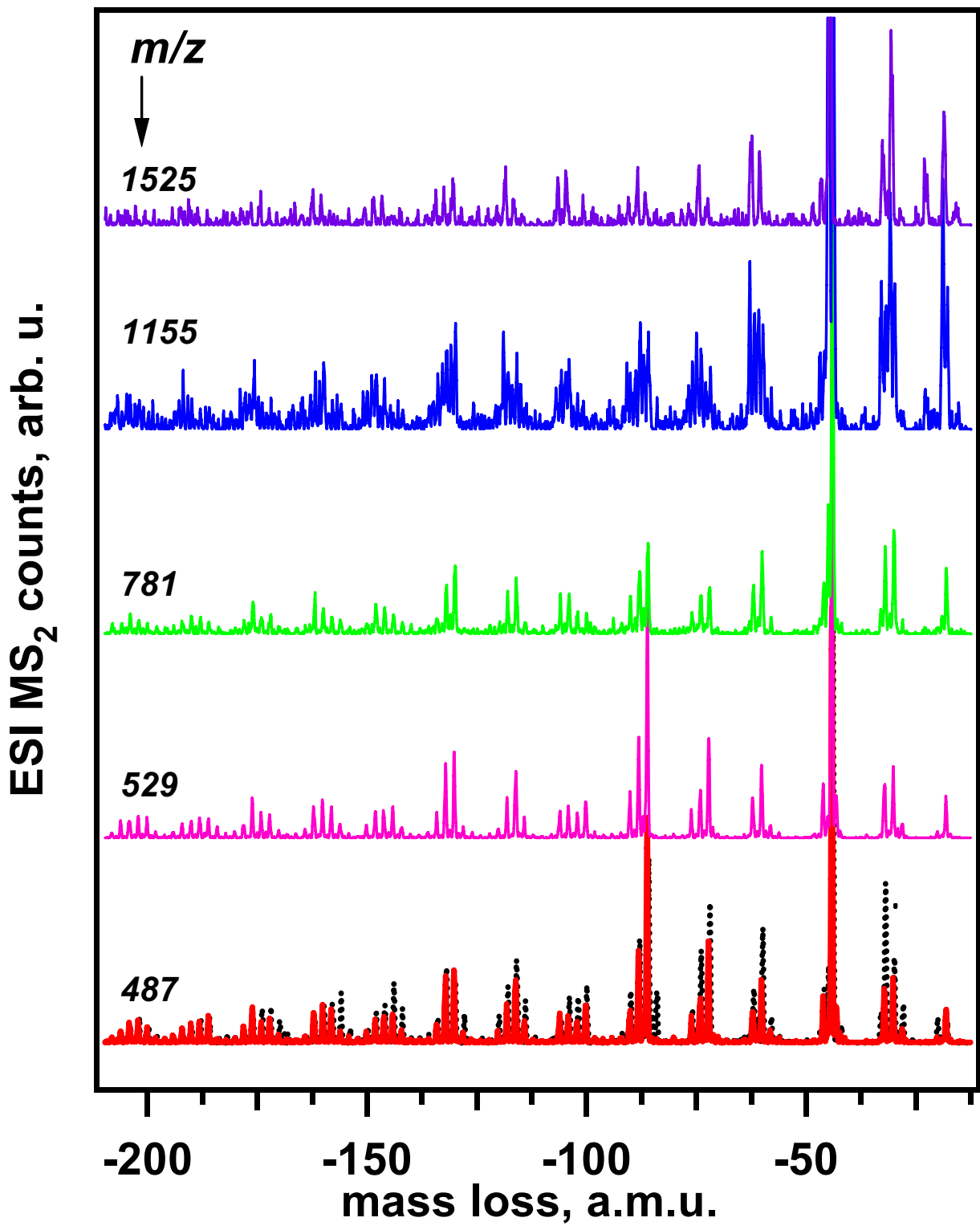


Figure 17S, Shkrob et al.

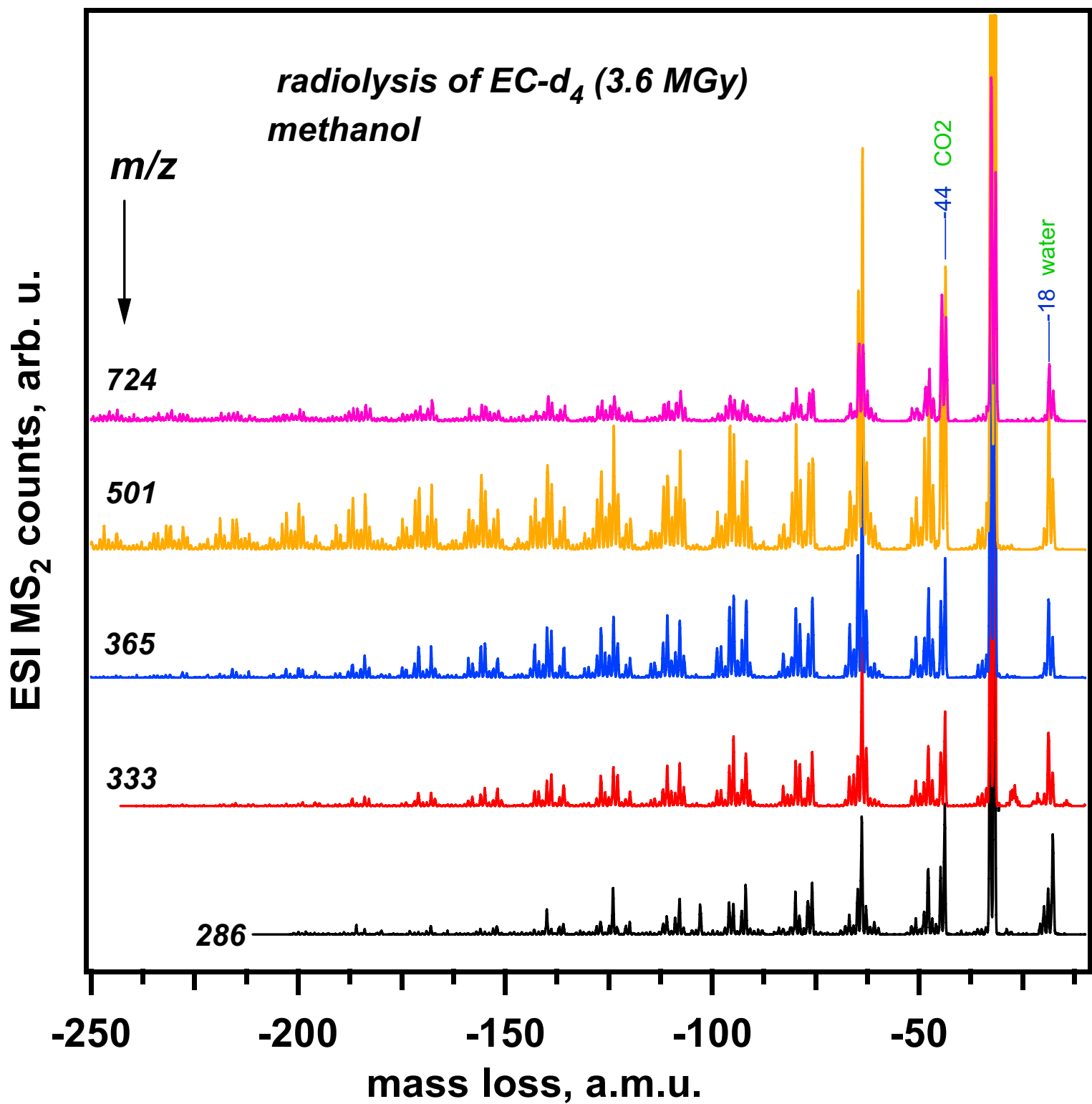


Figure 18S, Shkrob et al.

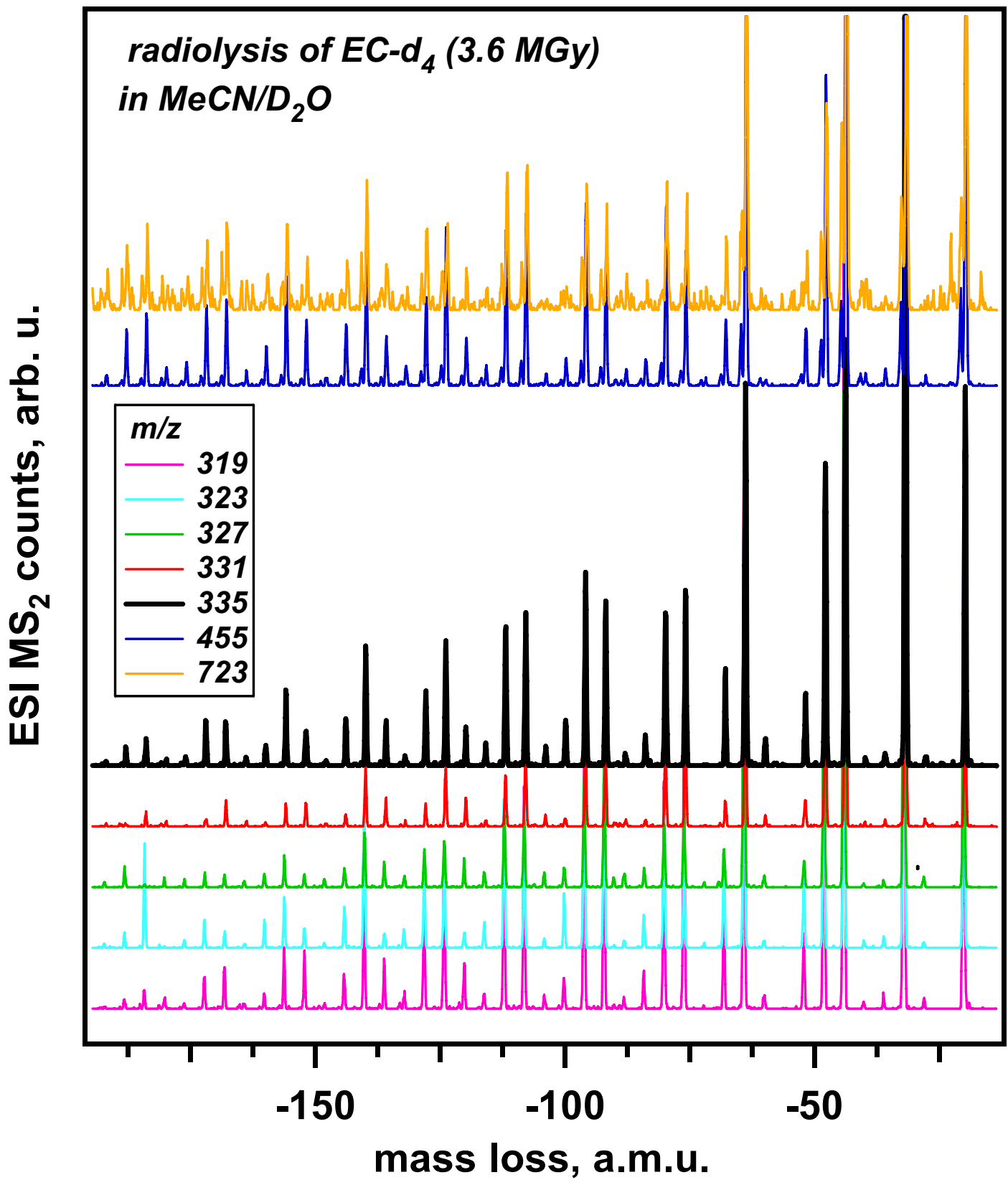


Figure 19S, Shkrob et al.

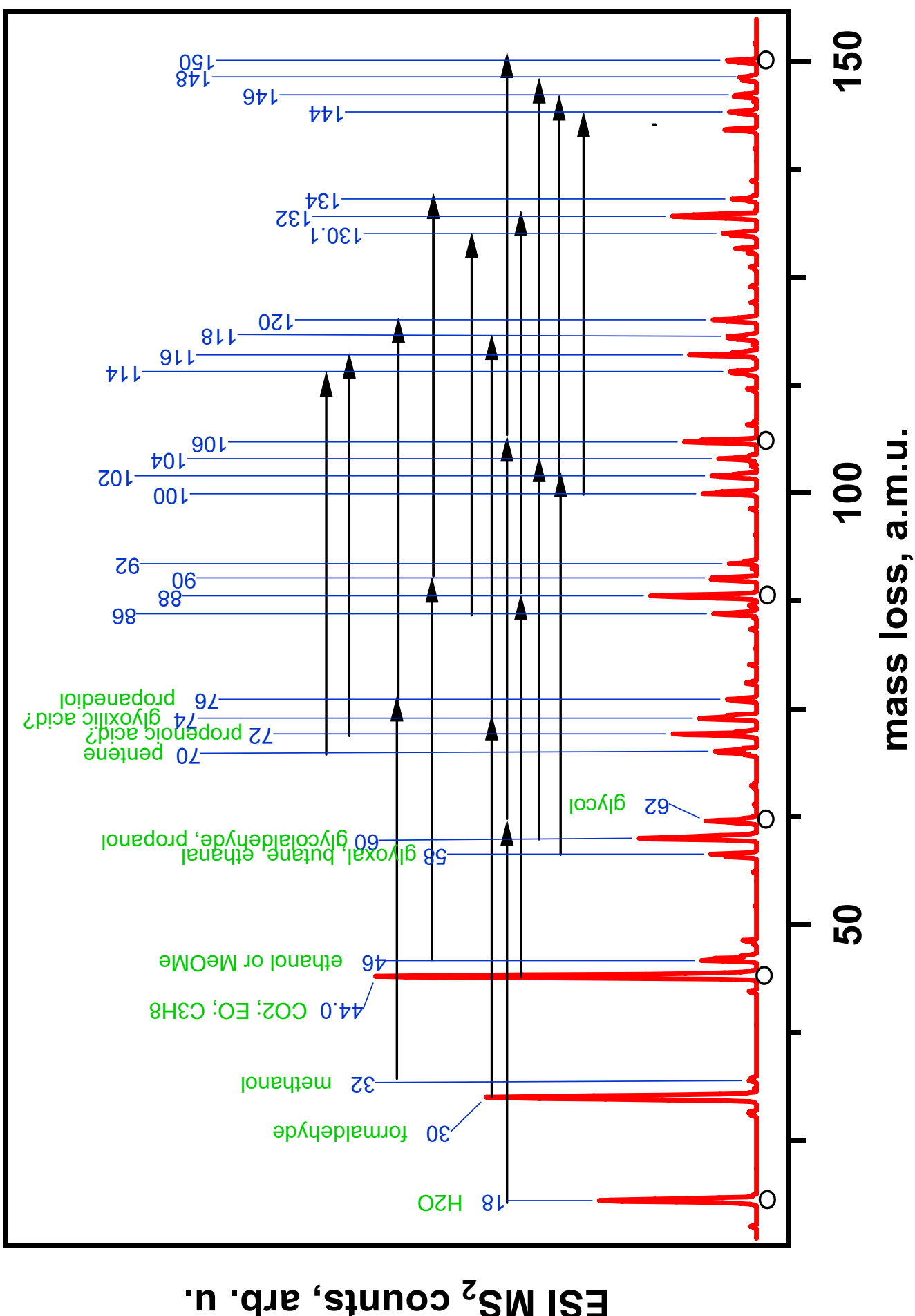
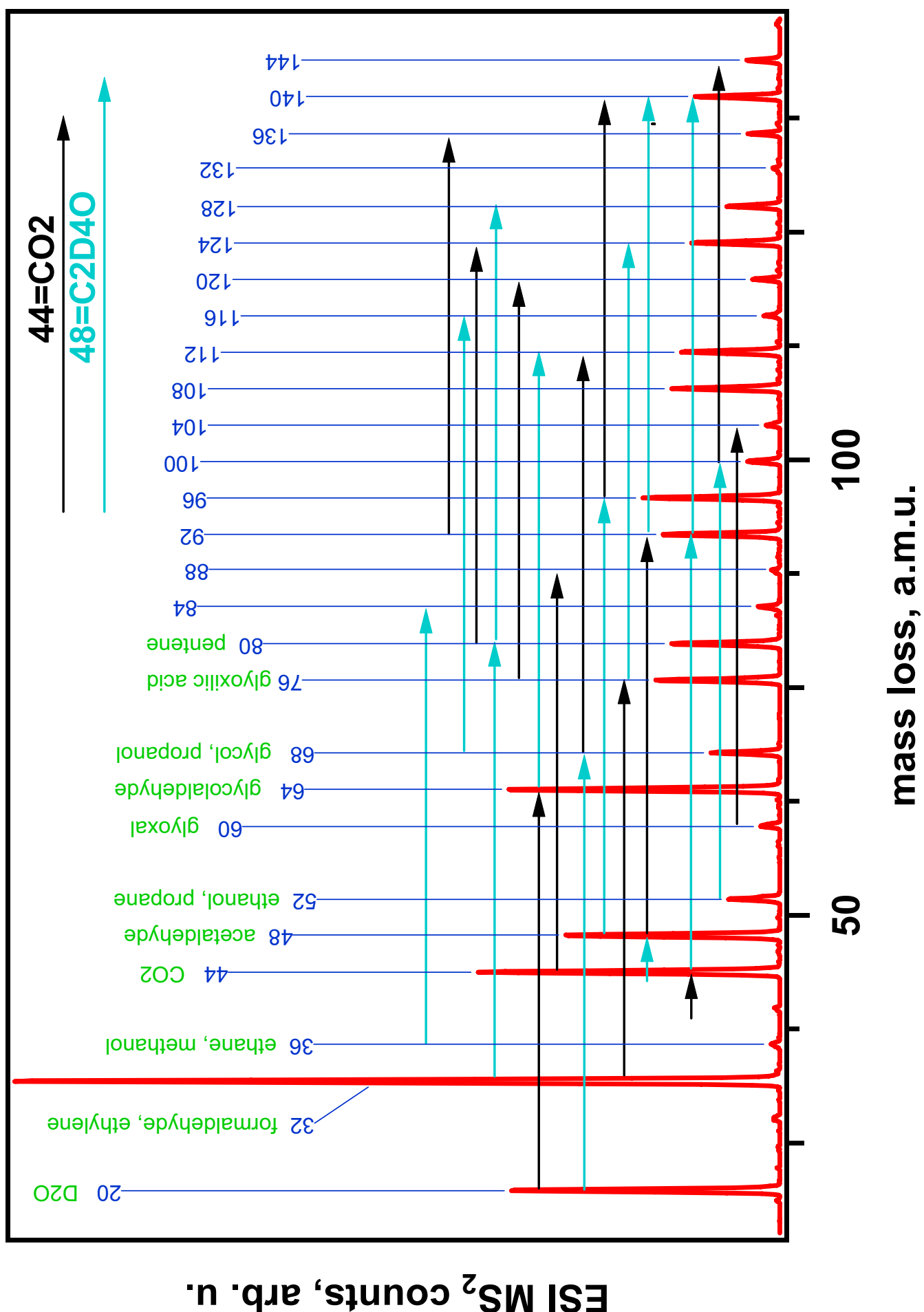
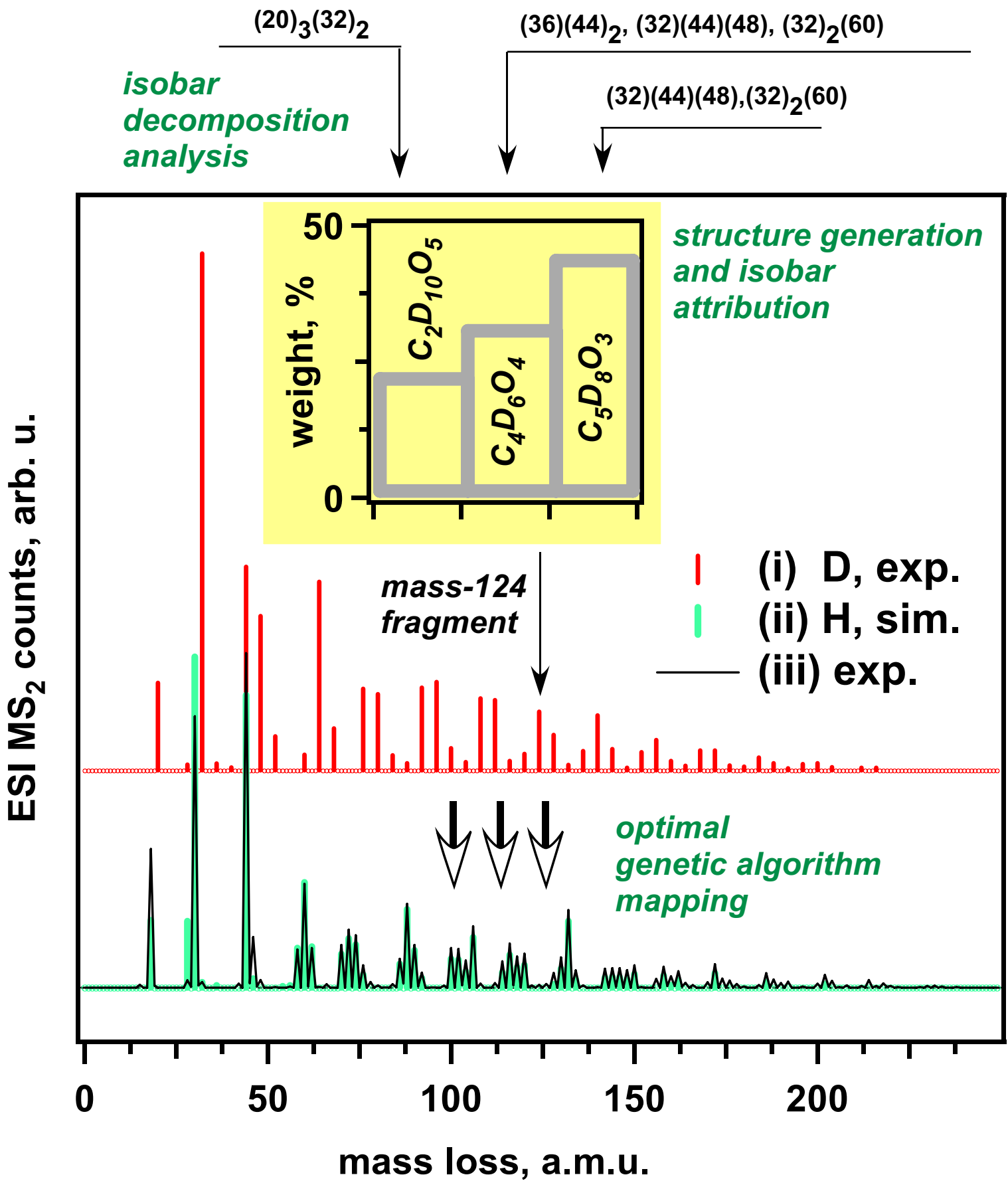


Figure 20S, Shkrob et al.



**Figure 21S, Shkrob et al.**



**Figure 22S, Shkrob et al.**

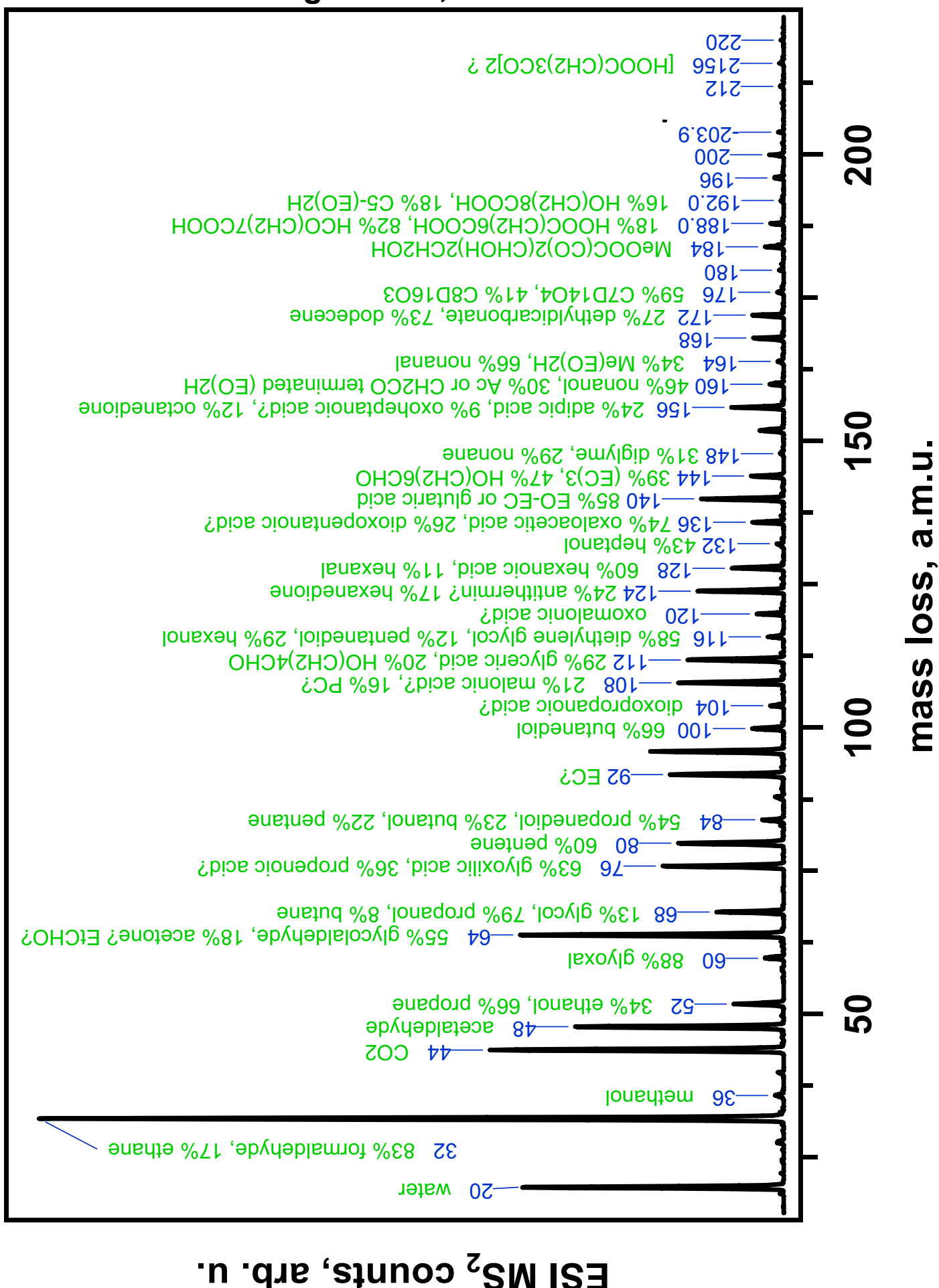


Figure 23S, Shkrob et al.

$^{13}\text{C}$  NMR spectrum of irradiated EC: part 1 of 2

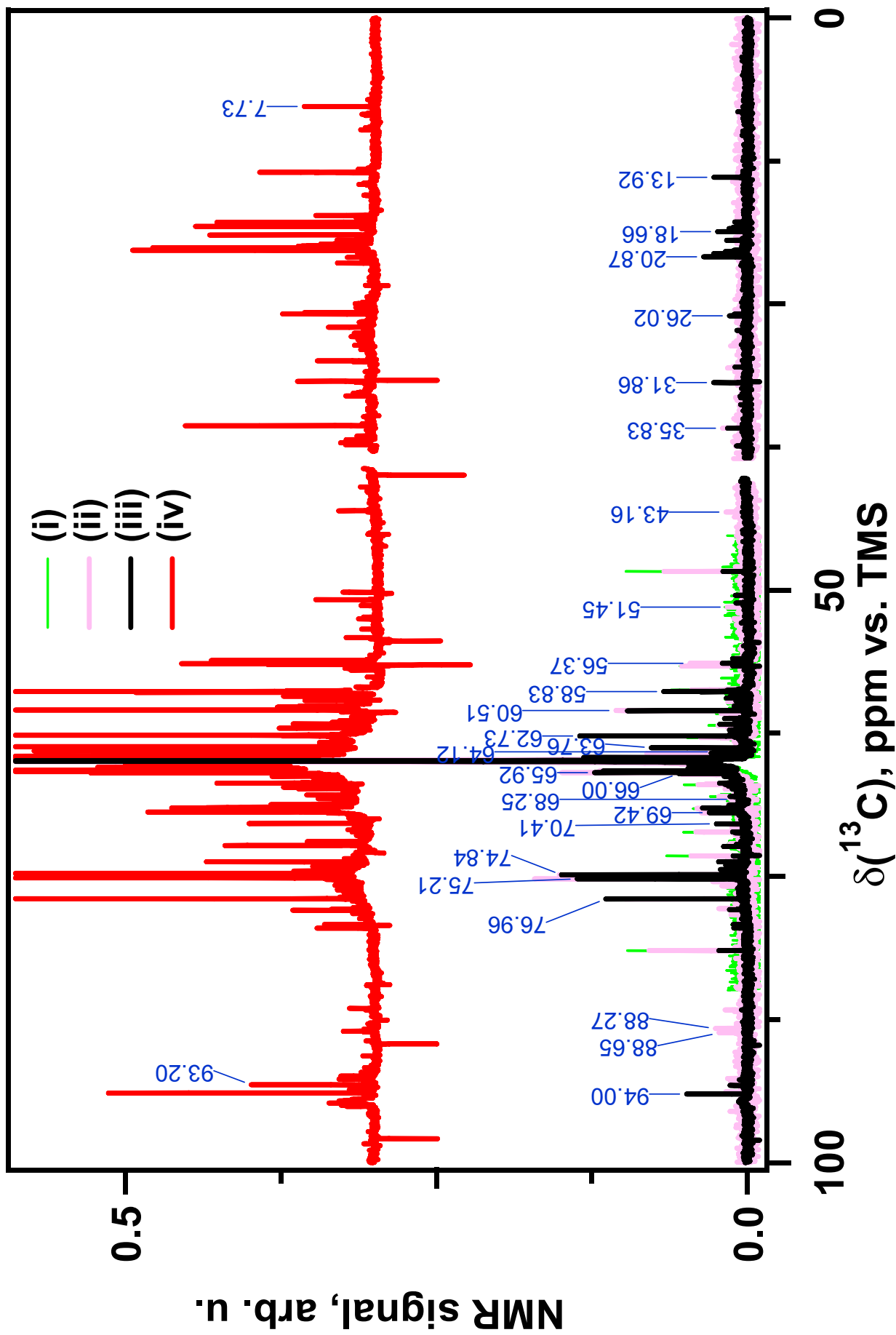
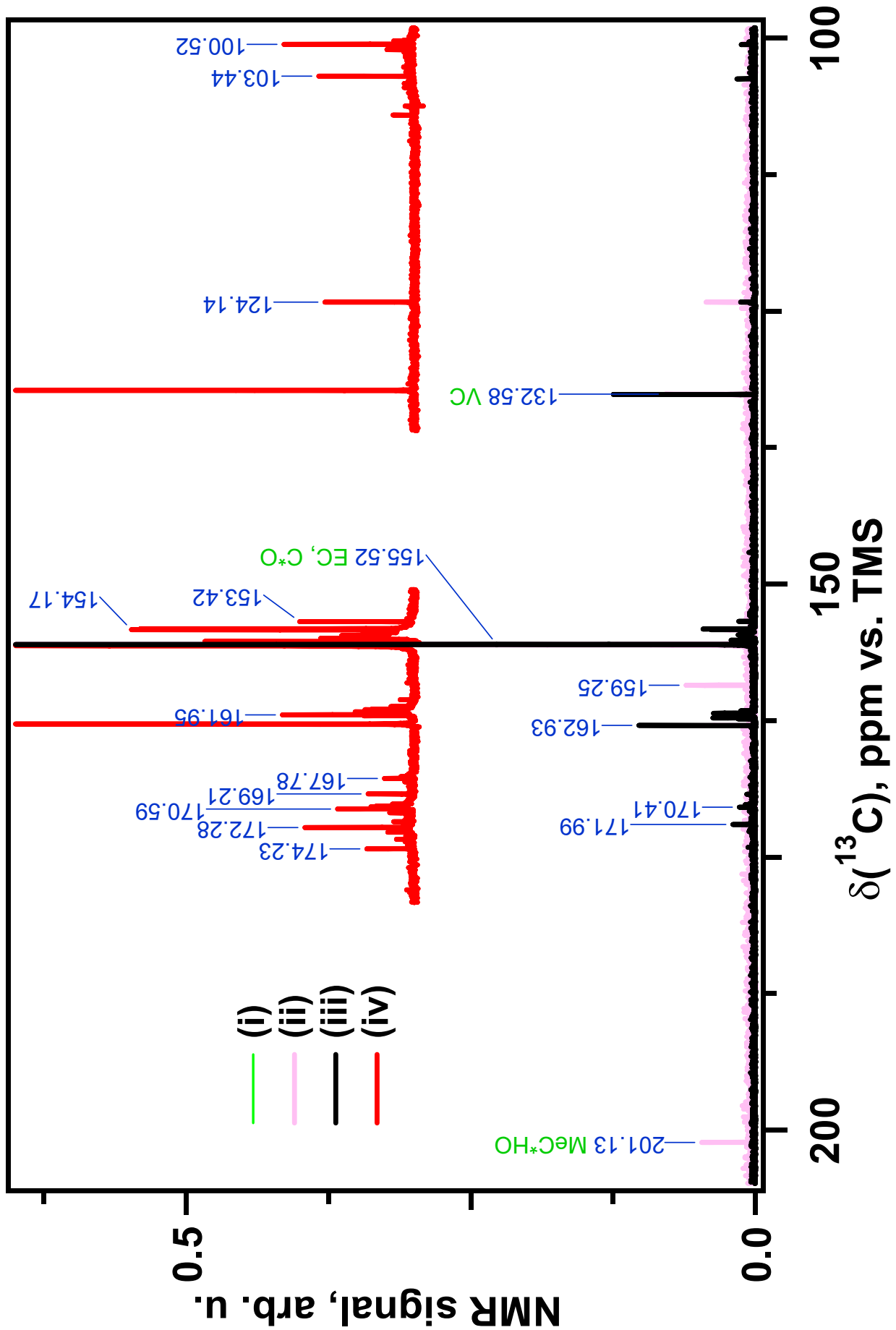


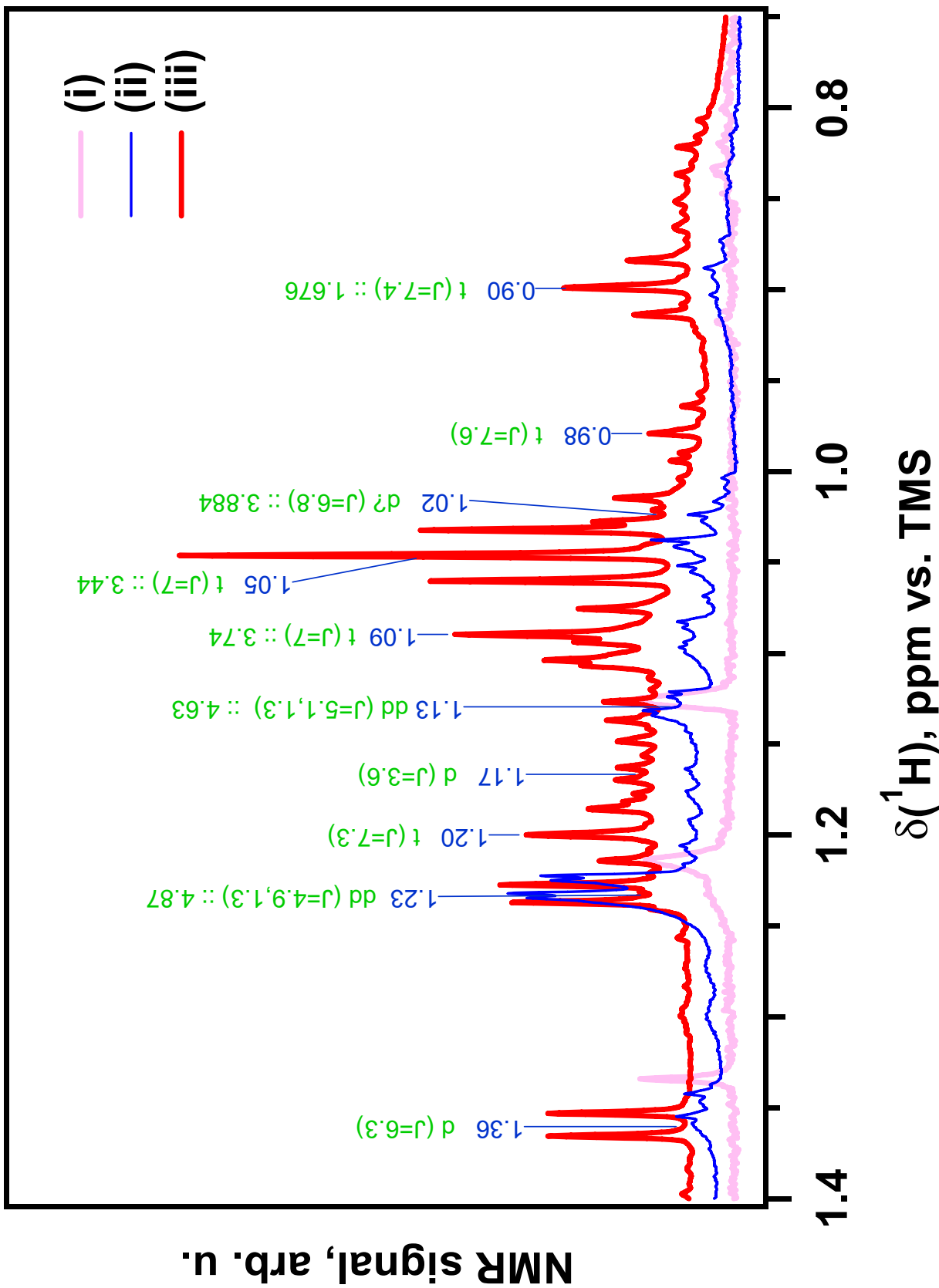
Figure 24S, Shkrob et al.

$^{13}\text{C}$  NMR spectrum of irradiated EC: part 2 of 2



**Figure 25S, Shkrob et al.**

**$^1\text{H}$  NMR spectrum of irradiated EC: part 1 of 6**



$^1\text{H}$  NMR spectrum of irradiated EC: part 2 of 6

Figure 26S, Shkrob et al.

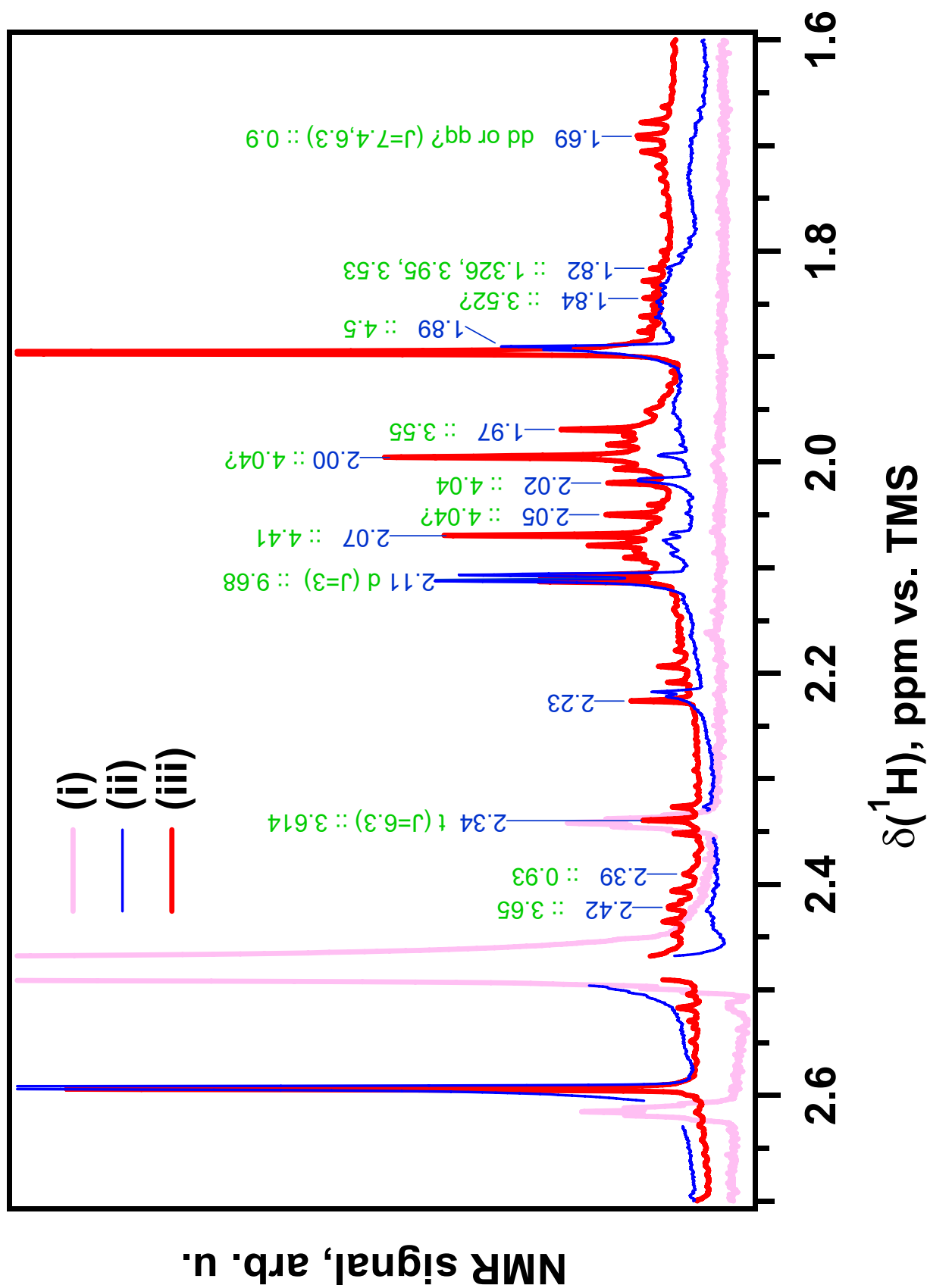
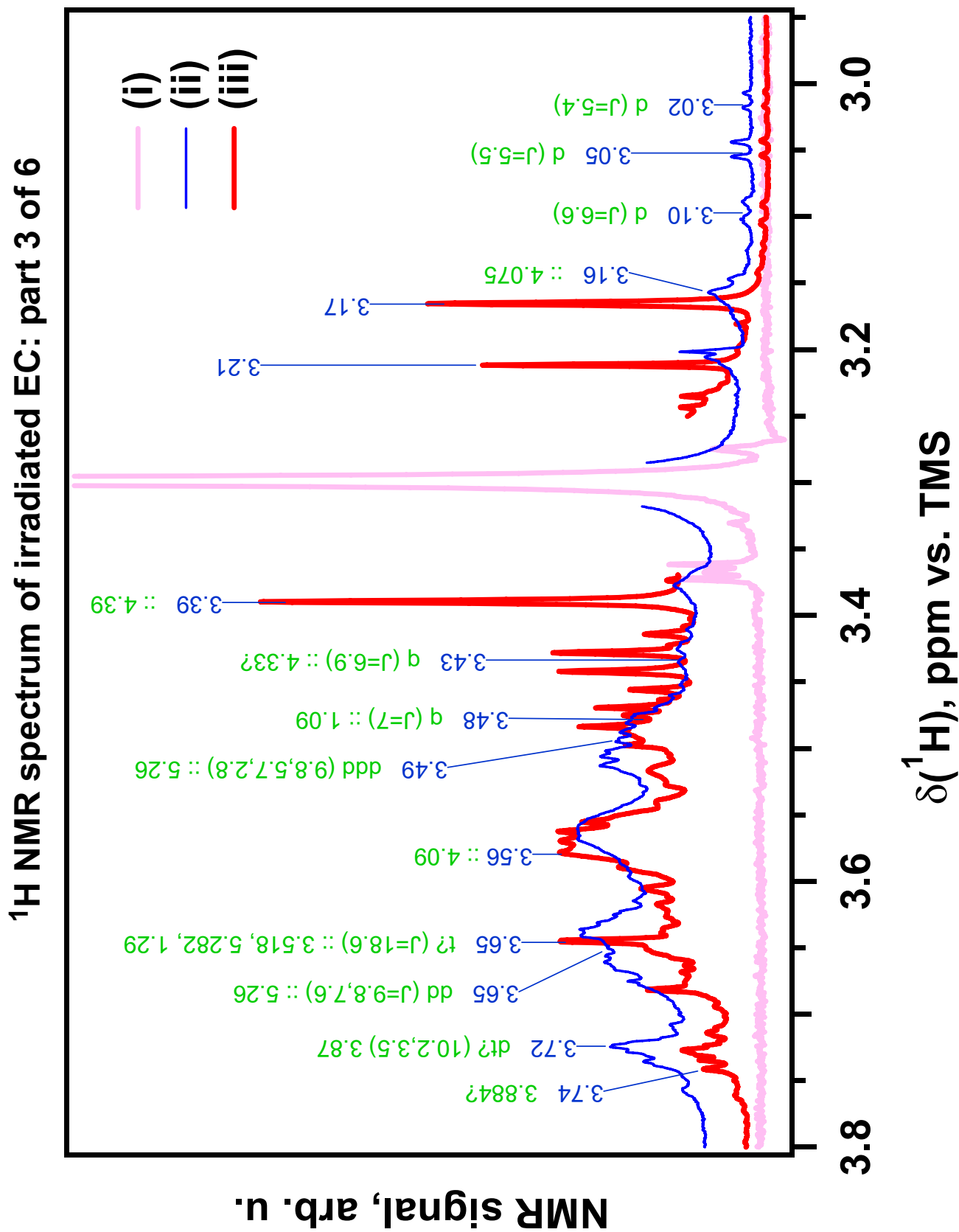
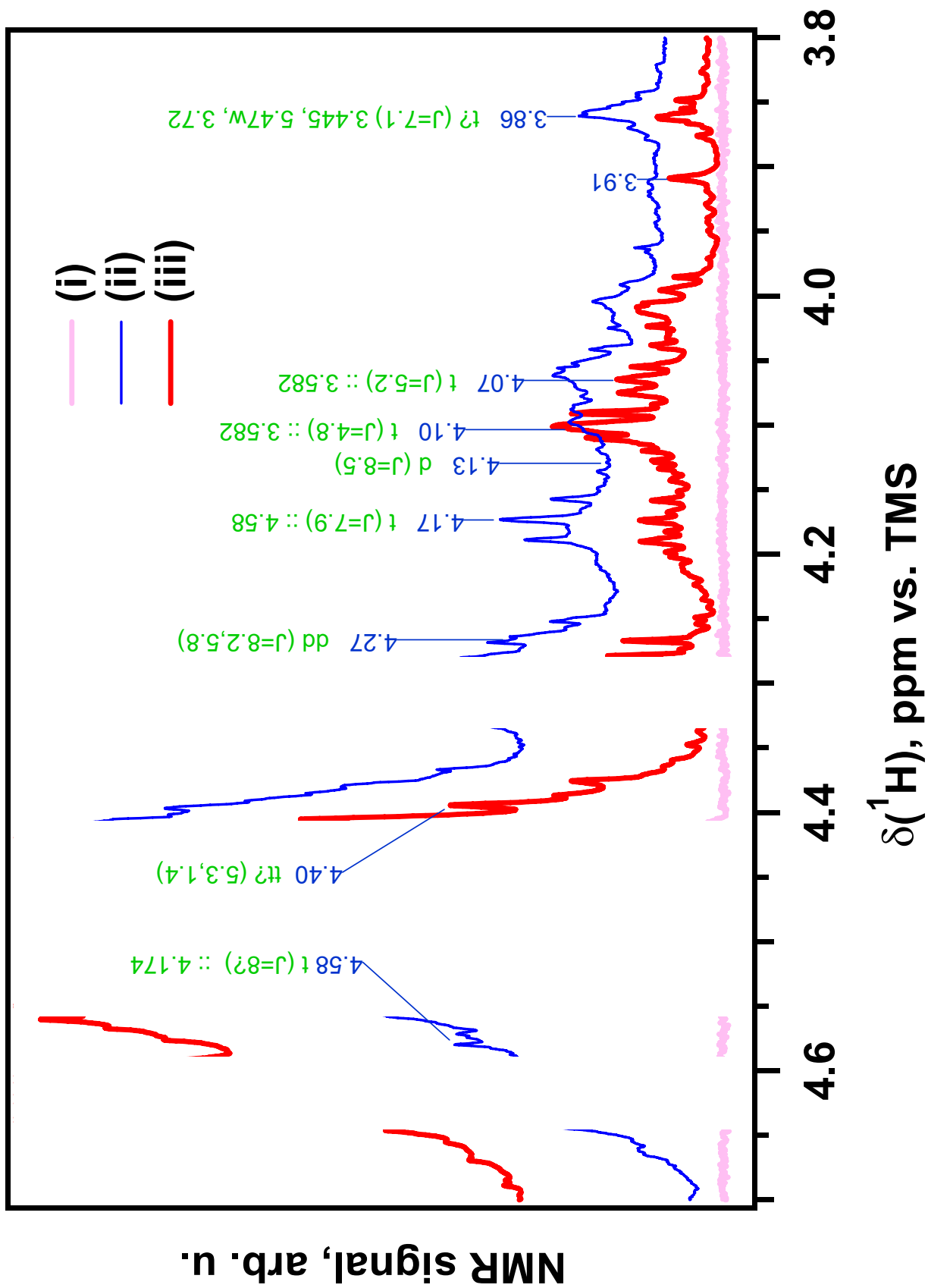


**Figure 27S, Shkrob et al.**



$^1\text{H}$  NMR spectrum of irradiated EC: part 4 of 6

Figure 28S, Shkrob et al.



**$^1\text{H}$  NMR spectrum of irradiated EC: part 5 of 6**

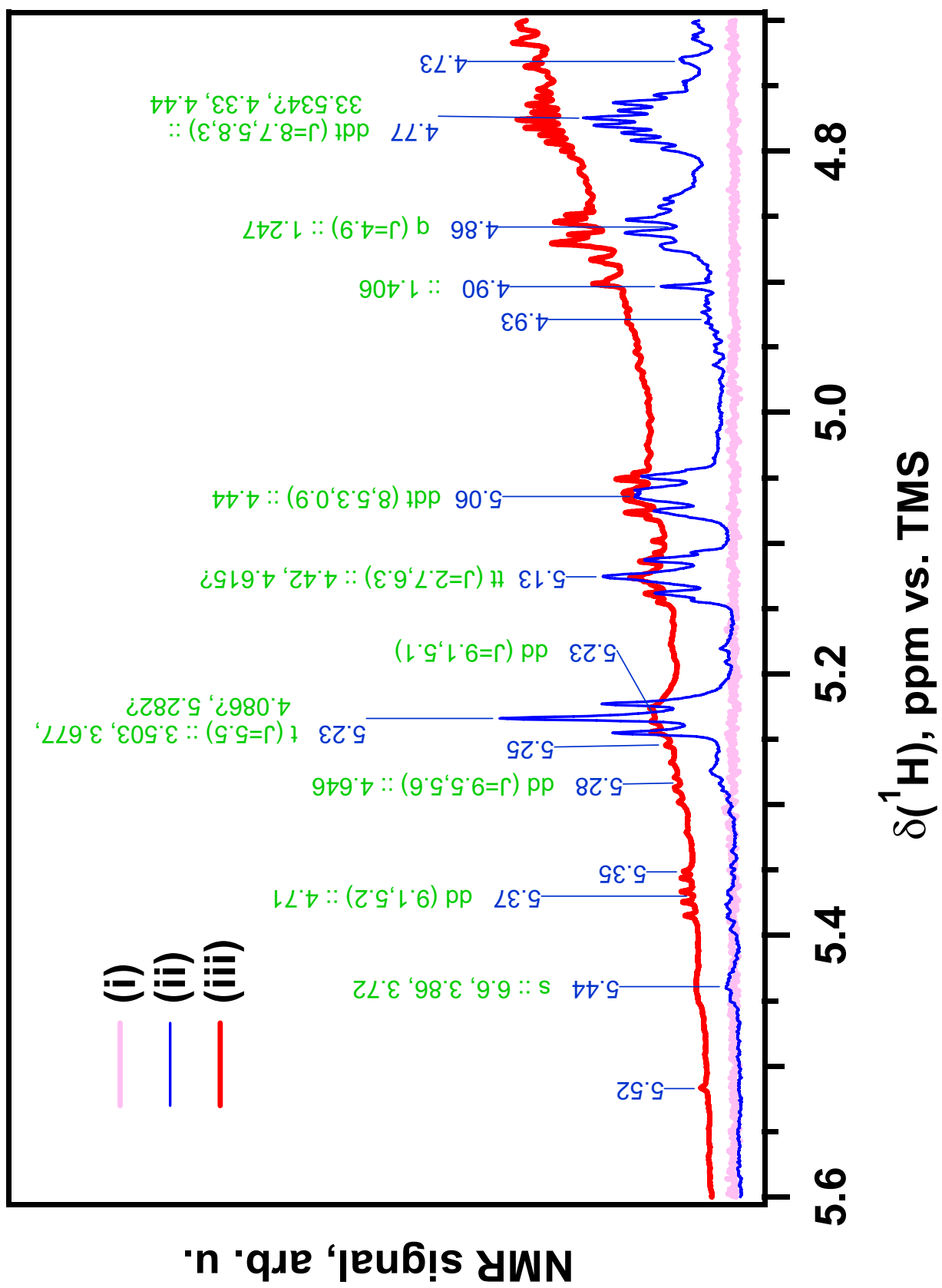


**Figure 30S, Shkrob et al.**

$^1\text{H}$  NMR spectrum of irradiated EC: part 6 of 6

